# Authors' response

We thank the three reviewers for the comments and appreciate their suggestions which improved the manuscript. In the following, the comments from the referees are included (in black) as well as our response (in blue). Additionally, we provide a marked-up version of the manuscript.

## Reviewer #1

Review of "Seasonal resonance of diurnal coastal trapped waves in the southern Weddell Sea, Antarctica" By S. Semper and E. Darelius

The authors provide observational evidence for large amplitude diurnal tides on the Weddell Sea slope, and then they seek to rationalize this finding in terms of resonant (zero group velocity) coastal-trapped waves. They go on to demonstrate the conditions (notably mean flow and stratification) that can make the resonant frequency vary from time to time. Overall, this is a credible piece of work, although there are perhaps some places where a bit more could be done.

The main extension I see would be to look at records from the same (or nearly so) isobath, but separated alongshore. These pairs can then be used to estimate alongshore wavelengths. This makes the most sense when moorings are simultaneous, but even if they are not, differences in Greenwich phase could be used to see if the estimated wavelength is at least the right magnitude. Also, the model results provide other information, such as direction of current vector rotation and amplitude of current components, that could also be used to compare with observations. Maybe all we will learn is that things have the right magnitude, but it could be more rewarding.
Reply: We included calculations of the wavelength for the two pairs of simultaneous moorings from nearly similar isobaths in the data set: M1–M4 and M2–M5. They suggest wavelengths of 250–600 km, with a larger range of 200–1600 km for $O_1$ during austral summer. This is roughly consistent with the wavelengths obtained for tidal frequencies in model runs that allow for tidal CTWs, although the RF wavelength typically is higher (>1000 km).
The direction of current vector rotation from the numerical code can be seen in Fig. 12 (background colours); the direction changes on the continental slope and the rotational direction is consistent with what the observations suggest. The amplitude provided by the numerical code is arbitrary and can therefore not directly be compared to the observations.

I recall reading somewhere that a PhD thesis by M. Spillane (Oregon State, 1980) showed that the wave dispersion curves can do strange things when inviscid group velocity vanishes. However, I do not know of anything quite like this is the normal literature. It would be interesting to know more about this but it would be asking too much to have this effect covered in this submission.
Reply: We had a look at the PhD thesis you mentioned. You are right, there is a figure of dispersion relations for viscous-damped free shelf waves for different Ekman depths where a singularity occurs at the resonant frequency. However, we have not seen this behaviour being reported in any other publication, and we agree that a more thorough investigation of this effect is beyond the scope of the work here.

Some specific points

- Line 37: Given the mooring notation, it is particularly important here to use the correct (subscripted) tidal notation consistently, e.g., is this M_2 or M2? (Yes, it IS clearly done right in other places).
Reply: Indeed, here the tidal constituent $M_2$ and not mooring M2 is meant. The typo has been corrected.

- 95: Please say more about the CATS tidal model. Is it barotropic? Does it include non-tidal currents? Is it nonlinear? Etc.
Reply: You are right, here is more information needed. We explained the CATS model more detailed now (see also the comment LP12 in the supplement from review #2): "Diurnal tidal KE has also been inferred using tidal predictions from the Circum-Antarctic Tidal Simulation version 2008b (CATS2008b), an updated version of the linear tidal inverse model described by Padman et al. (2002). The barotropic currents at the specific tidal frequencies are predicted for the respective time and location of every mooring deployment and are treated in the same way as the observational current velocities."

- 121: Say here how thick the boundary layer is.
Reply: The boundary layer is more than 25 m thick, as we see its effects at the lowest measurement level at 25 m.a.b., but not at the instrument level above which varies from mooring to mooring (55 m.a.b. for mooring M5, 442 m.a.b. for mooring M4, see Table 1. The text has now been changed to: "The energy associated with the diurnal tidal currents, the diurnal tidal KE (Sect. 2), shows little variation with depth, except at the

lowest measurement level at 25 m.a.b. In this bottom boundary layer, the diurnal tidal KE is slightly decreased compared to the overlying water column (Fig. 4). Depth-averaged diurnal tidal KE is used for further analysis."

- Page 5: Why normalize tidal KE? You are throwing out useful information (actual amplitude), and I do not see any advantage for normalizing.
Reply: In Figure 5a (now 6a), we normalised tidal KE to illustrate and compare its seasonal pattern better, i.e. the asymmetry between summer and winter maxima. The actual amplitudes are given in parentheses in the legend; the summer maximum varies from 10 $cm^2\,s^{-2}$ at mooring M5 to 203 $cm^2\,s^{-2}$ at mooring M3. Because of this large spread (resulting from the different locations of the moorings on the deeper slope, the shelf or at the shelf break), we decided to normalise tidal KE.

- 170: The evidence here on ambient currents vis a vis waves is pretty weak. True, you can say that the "mean" alongshore currents vary with time, but, evidently useful local information about the time dependence and the spatial structure is lacking. There is nothing you can do about this, of course, but it would be well to advise the reader that the main thing you can glean here is the magnitude of the "mean" flow, and that it (probably) does vary from time to time.
Reply: In this paragraph, we review what is currently known about the slope current and its seasonal variability upstream, and extend the description with information from our moorings. We have now a) included mean currents in Fig. 1, b) provided information about seasonal variability in the text and c) added a final statement summarising the results that can be used in the modelling: "The limited observations available from our study region suggest a westward flowing jet, which is relatively narrow and appears to be centred at the shelf break. The jet intensifies and widens during early austral winter."

- 243-244: This sentence does not make sense to me.
Reply: We compare the sensitivity of the RF for a change in current core location to a change in current core velocity, since the latter is shown in Fig. 10. We rewrote the paragraph for clarification: "The magnitude of the change in RF for a 40 km off-shore shift depends on the width of the current, but it is comparable to a change in current velocity of $\pm 10\,cm\,s^{-1}$ (Fig. 11)."

- 264: I am not sure what is meant by a dispersion curve showing the waves to be barotropic. There must be a missing step in the argument here. Maybe they mean the

modal structure (Fig 11) is barotropic? Also, give a representative range of Bu. It is probably a wording issue, but the last sentence of this paragraph seems to contradict the preceding text.
Reply: Yes, the modal structure (Fig. 12) and the observed values of tidal KE (Fig 4) show barotropic motion – as suggested by the low Burger number. We now provide an estimate of $Bu$ and the quantities used to calculated it. Results from the numerical code show however, that while the motion is close to barotropic, the dispersion curve is sensitive to relatively small changes in stratification (Fig. 9-10).

- 270: Enhanced relative to what?
Reply: We added "compared to austral winter" to the sentence to make it clearer.

- 272: What asymmetry is that?
Reply: We meant the difference in amplitude of the summer and winter maximum (see Fig. 6a). The text has been rewritten.

- Figure 7: Label axes.
Reply: It is unclear which axes the reviewer refers to. All axes are labelled in Fig. 7a (now 8a), while Fig. 7b (now 8b) is a schematic illustration of the parameters changed in the sensitivity test and has therefore no scale or units for the axes.

Again, I believe that this contribution is sound overall, but that improvements ought to be made.
Thank you!

## Reviewer #2

This paper is a comprehensive assessment of the seasonal variability of diurnal tidal currents in the southern Weddell Sea, using data from 29 moorings between 1968 and 2014. While the seasonal variability is known, and has been previously interpreted as response of diurnal tide-forced shelf waves to changing stratification and along-slope current (various papers from the 1980's), the increased data base and interpretation through sensitivity tests on an idealized model (Brink, 2006) makes this a valuable new study.

My specific comments are provided as margin comments and edits on the marked *.tex file. Most of these are relatively minor. Some major comments are as follows:

1. Lines 43-55, about CTWs, will possibly make no sense to a lot of readers without a dispersion curve to look at. Probably this means adding a simple sketch of one, showing that cp is always with shallow water on the left (in the Southern Hemisphere), then three cases of cg (+ve, -ve, and 0 (RF)).
Reply: We have included a schematic as suggested to complement the text.

2. Much of the Discussion is actually Introduction (Background) material. Move everything you knew, or should have known, before the study into Introduction. Discussion could keep some implications (regarding sea ice, mixing etc) that depend on the magnitude of the results you have presented, but expectations should be set in Introduction.
Reply: We have moved the background material from the discussion to the introduction as suggested. This involved some rearrangements in the discussion section.

3. The discussion of Figure 5 is not very clear. I think the argument you are trying to make is that the "diurnal band" as a whole shows mainly semi-annual, which you ascribe to K1/P1 modulation. Then, K1 (removing P1 influence by inference) is "annual". But the modulation of the diurnal band at the semi-annual frequency is too large for K1+P1, even without the other tidal lines (e.g., O1) being caught in the definition of "diurnal band". Some more thought about this, and an improved discussion, would be useful. It is not impossible that currents and stratification add to a semi-annual term in CTW properties.
Reply: We have discussed this point with L. Padman, and the comment is partly due to a mis-reading of Fig 5a (now 6a), which shows KE, and not tidal amplitude as L. Padman first thought. To show that the K1+P1 interference can explain the semi-annual signal we observe, we have included time series of KE obtained from CATS2008b (Fig. 6b). The observed semi-annual modulation of about 0.3-1 is in the upper range of what can be expected and can to a large extent be explained by $K_1$+$P_1$ modulation. We now discuss other potential contributors – as suggested by L. Padman – to the semi-annual modulation in the discussion.

4) What does it mean to have a wave whose wavelength (∼1300 km) is an order of magnitude longer than typical along-slope scales of isobath variability?
Reply: While this is an interesting question, it is beyond the scope of the current study. We now mention this in the ms, and note that the CTWs modelled by Skardhamar et al. (2015) similarly have wavelengths which are considerably larger than the topographic

scales. A full 3 D-analysis, similar to the one by Skardhamar et al. (2015), would be needed to fully explore the effect of bathymetry on CTWs in the study region.

– Laurie Padman

Please also note the supplement to this comment: http://www.ocean-sci-discuss.net/os-2016-36/os-2016-36-RC2-supplement.pdf

**Supplement**

Thank you for your thorough reading and the comments. The replies to the supplementary comments are given below and are kept rather short, as the comments are.

LP1: The tide-forced CTW's *are* tides; so maybe better here to say "Near-resonance of diurnal tidal CTWs during ..."
Reply: You are right, it might have been confusing. We followed your suggestion and rewrote the sentence.

LP2: I think the Introduction needs to include Nicholls et al., 2009 Reviews of Geophysics. Also, a lot of Discussion should really be moved to Introduction. Anything relevant that you knew or should have known before starting the study should be in the Introduction.
Reply: We now refer to Nicholls et al. (2009) as suggested, and we have moved parts of the discussion into the introduction (see also your comment 2 in the main review).

LP3: Seems to ignore the HSSW contribution to AABW formation.
Reply: While HSSW descends the slope and contributes to AABW formation farther west in the Weddell Sea, ISW is the main contributor in our study region. But ISW is again HSSW+meltwater, so including both water masses (while keeping the text short), we now write: "This is where cold and dense water masses, formed on the continental shelf and underneath the Filchner-Ronne Ice Shelf (FRIS), cross the shelf break and descend the continental slope (Foster and Carmack, 1976; Foldvik et al., 2004; Nicholls et al., 2009).

LP4: Strange sentence. What about the inflow and outflow are "influenced", vs "to some extent set" ? And how do these two things even differ?
Reply: There is no real difference, so we reworded the sentence: "Physical processes at the shelf break and on the continental slope influence both the cold outflow and the warm

inflow in terms of their hydrographic properties and strengths."

LP5: Note sure I got the TeX right, but just include Darelius as a regular cite.
Reply: It is a TeX thing (our key name for this article).

LP6: You need to explain the source of the mixing better here. I think you are referring to bottom stress. If you want to claim a baroclinic source of mixing, then needs a cite. Fer et al. paper in prep. would be good, but maybe Ilker's Yermak Plateau paper?
Reply: Yes, this was unclear. We included two references and rewrote the sentence: "Mixing can be expected to be further enhanced at the shelf break by the strong diurnal tidal currents (Fer et al., 2015; Pereira et al, 2002)."

LP7: I think this discussion will not make much sense to most readers until you show a dispersion curve for a CTW, even if it is just a schematic showing cp (always shallow water on left), and the three cases of cg>0, cg<0, and RF.
Reply: See your comment 1 in the main review.

LP8: This expression isn't clear; probably need a little introduction to bathymetric irregularity, convergence etc.
Reply: This is a good point; the reader should get a slightly more detailed explanation. We rephrased the sentence: "In practice, energy likely escapes in one or the other direction along the slope. Leakage of energy occurs for example because of irregularities in the bathymetry and because the bottom slope changes (i.e. isobaths converge or diverge, Thomson and Crawford, 1982). Therefore, we use the term near-resonance rather than resonance."

LP9: This approach is sensible, but relies on choosing a length scale for the calculation of local isobaths orientation.
Reply: See comment by reviewer #3.

LP10: Better word than "chunk" ? Maybe "intervals" ?
Reply: Agree, "intervals" is a better word. We changed the paragraph accordingly.

LP11: So, how long is each window? I think this needs 3/4 of a month to work, but that is a bad window length for tides. Better to use 14 or 29 days (more precisely, the spring/neap for O1/K1)

Reply: Sorry for the confusion. The window length we used is 14 days (a third of 1.5 months), but since they are overlapping, there is actually five windows within each interval. We corrected the paragraph: "The hourly-averaged current meter data are divided into intervals of 1.5 months length beginning every 14th day. For each interval, the power spectral densities are estimated using Welch's method (Welch,1976) and 14 day long, 50 %-overlapping Hanning windows."

LP12: Need to be clear about which version of CATS you are using. The cite you give is for CATS, or CADA00.10, both very old. I think you use CATS2008. If so, the cite would be
"... Simulation version 2008b (CATS2008b) an updated version of the tidal inverse model described by Padman et al. (2002)."
Reply: Yes, we are using CATS2008b, but did not know how to cite it properly. Thanks for correcting this!

LP13: This is probably good, but it seems a little bit strange since the energy in the tide model is known exactly for exact frequencies.
Reply: We are aware of this, but decided to treat both observational and model data in a consistent way.

LP14: Mike Foreman did the really hard work here!
Reply: Thanks for pointing this out, we were not aware of this! We followed your suggestion and cited his work.

LP15: 1) I guess you don't do much with the semidiurnals, but you'd also need to use inference to separate S2 and K2.
2) Inference on K1/P1 assumes that the relative amplitude and phases are constant throughout the year. Given sensitivity of actual CTW currents to exact frequency, is this valid?
Reply: 1) Correct, we do not do anything with the semidiurnal tides, so we did not see the need for separating S2 and K2. 2) We cannot claim that the relative amplitude and phases are constant throughout the year. Hence, we removed the previous Fig. 5b where we used the separation of $K_1$ and $P_1$ and also removed the sentence in the methods you refer to here.

LP16: Topographic setting is the key to CTWs, right? Not the outflow.

Reply: Right. We changed the sentence following your suggestion.

LP17: Figure 3 caption needs to tell us the water depth for each of M5 and M4.
Reply: Thanks, that is a good idea. We changed the caption to "Diurnal tidal KE over time and depth at a) mooring M5 and b) mooring M4 on the continental slope, located above the 1900 m and 1050 m isobath, respectively."

LP18: This figure needs two panels, one for summer and the other for winter.
Reply: We do have a similar figure for austral winter, but decided to not show it. Since the area of the circles is proportional to the square root of the maximum of depth-averaged, diurnal tidal KE, the summer–winter differences are not easy to see. Here we rather want to show the spatial distribution of maximum tidal KE.

LP19: You need to talk about what it looks like *west* of the trough, which is different from east of the trough. Otherwise, it looks like you are hiding something. (Are you?!)
Reply: No, we are not trying to hide anything. At moorings A and B2, the major axes are directed mostly across-slope, similar to the eastern part of the study area. For the F-, D-, and W-moorings, the picture is more complicated. They are located close to the ridge which might influence both the accuracy of the chosen rotation angle and the tidal currents over this bathymetric barrier. We rewrote the sentence: "The major axes of the tidal ellipses at the $K_1$ frequency are directed across the continental slope for moorings located at the shelf break and on the continental slope (especially for the ones east of the Filchner Depression and west of the ridge). Hence, the diurnal tidal energy is higher in the across-slope component than in the along-slope component."

LP20: Something is wrong here! P1 and K1 don't explain this high degree of semiannual variability, especially as the "diurnal band" still contains O1.
Reply: As explained in comment 3 in the main document, this comment is due to a misreading of the figure labels. Figure 5a (now 6a) shows diurnal tidal KE, not tidal amplitude. The semi-annual modulation by $K_1$+$P_1$ can to a large degree explain the observed signal in diurnal tidal KE.

LP21: This is a nice figure. However, is it really a "Hovmoller" diagram as stated in the caption? `https://en.wikipedia.org/wiki/Hovm%C3%B6ller_diagram`
Reply: Thanks. Yes, it is a Hovmöller diagram. Following your link, it says: "Hovmöller diagrams are also used to plot the time evolution of vertical profiles of scalar quanti-

ties such as temperature, density, or concentrations of constituents in the atmosphere or ocean. In that case time is plotted along the abscissa and vertical position (depth, height, pressure) along the ordinate."

LP22: I disagree: In your Figure 6, if I plotted T and S at the bottom of the plot, I would see a seasonal signal.
Reply: At mooring M3 shown in the figure (now Fig. 7), it is the thermocline that varies in depth over the year. It reaches the bottom during austral winter, which leads to the apparent seasonal signal you refer to. However, at moorings located farther down the continental slope (M5, for example), no seasonal signal is present below the thermocline. We changed the sentence to avoid confusion about this: "The deeper moorings (e.g. M5) show that seasonal changes in the water column below the thermocline are negligible (not shown)."

LP23: You don't really have a "level of the code". Really, all you need here is
Reply: This comment is incomplete, but we have removed the "level of the code".

LP24: If the wavelength is really this long, does it make sense to think of these as 'waves' when along- slope topography varies on much smaller scales?
i.e., Discuss implications for wavelength >> topo scales
Reply: See your comment 4 in the main review. We can not address this point with the tools at hand, but we note that the wavelengths of the tidal CTWs modelled by Skardhamar et al. (2015) also are larger that the scale of along slope variability.

LP25: It's been so long since you mentioned this, you might need to explain it again.
Reply: We are not in favour of re-defining abbreviations, but see your point and changed to: "For tidal CTWs to exist, the dispersion curve must pass through the tidal band, i.e. the maximum of the dispersion curve (the resonant frequency, or "RF") must lie within (thus giving near-resonance) or above the diurnal tidal frequency band."

LP26: So ... why not use higher resolution in the Brink model? This is the obvious thing to do. I know there are some stability issues with this code, and maybe that's the answer. But if this is the reason, you need to discuss it here, or maybe better in Section 4.1.
Reply: You are right, it is the stability issue that prevented us from simply increasing the resolution. We agree that we should discuss this, and did so in Section 4.1: "The code was set up using 30 vertical levels and 120 horizontal grid points to represent a 2 D-cross-slope

section. This is within the recommended range of grid points; increasing the resolution leads to instability and failure of the test for hydrostatic consistency."

LP27: Figure 10 needs O1 and K1 frequency lines marked.
Reply: This is a good idea. We included the $O_1$ frequency line only, as $K_1$ lies much higher (note the small scale of the y-axis).

LP28: I do not like this bracketed way of doing opposite cases. In general, you can ignore the bracketed examples as they are implied as the opposite of the main case. If that isn't true, then you'd need a clear sentence for the opposite case anyway.
Reply: Changed, see comment by reviewer #1.

LP29: I think you mean 'cf.', but use "compare the" instead
Reply: Yes, we meant cf. and changed it accordingly.

LP30: A lot of the Discussion is actually Introduction/Background, that should have told you what to expect before you got to the end. Almost every sentence with cites could have come earlier. As just one example, discussion of the Skarohamar et al. (2015) *model* result could have been used in the Introduction to point to 3-D model support for the more idealized analyses of, e.g., Middleton et al. 1987.
So, thin out the Discussion and strengthen the Introduction.
Reply: See your comment 2 in the main review.

LP31: 1) How does a dispersion curve show that the CTWs are relatively barotropic? I *think* the answer might be that Mode-1 is the only CTW Mode that can get close to diurnal frequencies, but the modal structure refers to the number of zero crossing across-slope, right? Not the vertical structure.
2) You then present a Burger number argument, which makes more sense, but is not explicitly related to the CTW dispersion curves. Better to just argue based on Burger number, or extract something from the Brink model that explicitly demonstrates that the mode(s) is(are) barotropic.
Reply: This was worded confusingly. See also comment by reviewer #1. The modal structure (Fig. 12) and the observed values of tidal KE (Fig 4) show barotropic motion – as suggested by the low Burger number. We now provide an estimate of $Bu$ and the quantities used to calculated it. Results from the numerical code show however, that while the motion is close to barotropic, the dispersion curve is sensitive to relatively small

changes in stratification (Fig. 9-10).

LP32: This is too vague. Be explicit about the magnitude of the "seasonal" variability you would expect from astronomical forcing (basically, what modulation do you expect from the K1/P1 couplet?) and state that it is semi-annual (Figure 5a) not annual (Figure 5b)
Reply: We now included a more comprehensive paragraph on the $P_1$-$K_1$-coupling (Fig. 5a, now 6a,b) and removed the previous Fig. 5b.

LP33: Mack et al., 2013, GRL, show nicely that sea ice responds to the tides (for the Ross Sea). Padman and Kottmeier, 2000, JGR (already cited) show tidal motion of ice for the Weddell Sea. If ice is mobile, it can't dissipate tidal energy; it is "free drift". It's ice mechanics at high ice concentration that provides the friction needed to reduce tides.
Reply: We included your information in the text.

LP34-36: All Introduction text
Reply: We rewrote the introduction and discussion, as you suggested in comment 2 in the main review.

LP37: Not the right cite. Various available, including Kowalik and Proshutinsky 1994, Padman and Kottmeier, 2000; Mack et al., 2013.
Reply: Sorry, you are right, this was a typo. Anyway it is good to include several references, which we did now.

LP38: I'm not sure why this figure only comes up in Discussion: seems like "Results" to me.
Reply: This figure illustrates the consequences or effects the strong diurnal tidal currents and CTWs have. To us, this seems to fit better in the discussion than at any place in the results.

LP39: Raising warm water above the shelf- break depth does not, by itself, do anything. *Ignoring friction*, CTWs just conserve vorticity; "the tide goes up, the tide goes down". So, the key to this being important lies in coupling, either with mean flows or friction. Or, as some people have studied, the rectified flows that arise from tidal interactions over sloping topography.
Your paper is not about these processes, and doesn't need to be, but this section needs a

little more information to avoid being misleading.
Reply: We agree that more information will help the understanding. We rewrote as: "The existence and strength of diurnal (and longer period, Jensen et al., 2013) CTWs in the region must hence be expected to directly influence the availability of warm water above the shelf depth, i.e. at depths where it can potentially access the continental shelf through the influence of other processes such as e.g. a background mean flow, rectified tidal flows, friction or eddy exchanges."

LP40: Yes? Even if not, specify exactly which one.
Reply: Indeed, we should specify the version of the tidal model CATS, which we did in the revised version of the manuscript (see LP41 & LP42).

LP41 & LP42: This is a bit unfair: CATS, like every other tide model, is a barotropic model with only tides included.
More honest to say
"... CATS2008 (Figure 11), which does not include stratification or the variability of mean circulation required to predict seasonal modulation of tidal current."
Reply: We agree, this was not formulated well, but was not intended as criticism against the model. We rewrote the paragraph following your suggestion.

LP43: In Conclusions, minimize acronyms even if explained earlier. If useful here, explain them again.
Reply: We followed your suggestion as earlier (LP25) and explained the acronym again.

LP44: Huh?! How can you say "likely" when you have no direct evidence of something? Maybe the problem here is mixing the diurnal wind forcing issue with the others. I think your conclusions are:
"No evidence for wind forcing of diurnal tidal currents."
"No evidence that sea ice affects the diurnal CTWs."
"Varying bathymetry east of the study area likely affects the CTWs seen in the study area."
However, varying bathymetry anywhere affects the CTWs, so why only comment here on the upstream?
Reply: You are right, this was confusingly formulated. We comment on the bathymetry in the east as it is much steeper there, i.e. there is a strong divergence of isobaths into the study area, while the differences west of the study area are less pronounced. We changed

the sentence to: "While no direct influence of wind on the diurnal tidal currents and no evidence of sea ice affecting the diurnal CTWs have been found, the varying bathymetry east of the study area likely affects the propagation of the CTWs."

## Reviewer #3

This paper deals with Diurnal Topographic Waves (DTW) in the Weddell Sea. The paper is motivated by mooring data collected over several decades and these are discussed on the basis of results from an idealized code of Coastally Trapped Waves. In general the paper is well written and should be suited for publication. There are however some points that the authors could consider prior to publication.

For completeness I miss a figure of the mean velocity based on the moorings, could this be added onto on of the figures? This is of relevance for the choice of current profiles across the shelf break, and further a seasonal variability of the current velocities could be discussed in terms of DTWs summer to winter difference.
Reply: This sounds like a good idea. However, most of the moorings are located in the Ice Shelf Water plume, which flows out of the Filchner Depression, and the velocities will be influenced by that (see Fig. 2 in Foldvik et al.,2004). We added the mean velocities of the moorings that are supposedly least influenced by the plume onto the map in Fig. 1 and included more information about current velocities in the results.

Specific comments:

Line 12: Use "weak stratification" instead of "low stratification"
Reply: Thanks for pointing this out. We changed from "weak" to "low" and checked the manuscript for consistency on this.

Line 72: Change to "(Brink, 2006) to investigate . . ."
Reply: Changed according to your suggestion, the sentence reads more easily now.

312-323: The authors conclude that the summer amplification of the DTWs during austral summer is not explained by wind. Is there a possibility that the opposite could be the case, i.e. that the increased storminess has a destructive effect on the DTWs during the austral winter?
Reply: According to Gordon and Huthnance (1987), short-duration storms have been

observed to excite near-resonant mode 1 CTWs. Wind is generally a means of forcing CTWs (Huthnance et al., 1986). We have not found any example for increased storminess having a destructive effect on CTWs, as you suggest. If there is any, we do not consider this effect to be large.

Line 54-55: Is there a reference to accompany this sentence?
Reply: We rewrote the sentence as follows, including a reference (see also comment LP8 in the supplement from reviewer #2): "In practice, energy likely escapes in one or the other direction along the slope. Leakage of energy occurs for example because of irregularities in the bathymetry and because the bottom slope changes (i.e. isobaths converge or diverge, Thomson and Crawford, 1982). Therefore, we use the term near-resonance rather than resonance."

Fig 1 and Fig 10: There might be some confusion about what is the positive along-slope current direction; in Fig 1 this would be toward the east while in Fig 10 this appear to be toward the west. Any particular reason why not having positive values with the coast to the left in all cases?
Reply: You are right, this is confusing. For the model set-up, a right-handed coordinate system is used where $u$ is directed on shelf, hence $v$ is positive eastward. We changed Fig. 10 such that the velocities are negative, to be consistent. However, when we mention westward flow in the text, we use positive amplitudes, as the term "westward" already contains information on the direction.

Line 80-85: More information is needed here, e.g. the calculation of the orientation of beta requires some choice of averaging length scale that needs some motivation.
Reply: The average length scale was chosen to be on the order of 10 km. An exact number is difficult to provide, as a useful length scale also depends on the location of the mooring (i.e. shorter scales for moorings close to the ridge where bathymetry changes more). All angles have been checked visually to insure consistency. The text has been changed to: "The rotation angle $\beta$, positive for clockwise rotation, is listed in Table 1; it is inferred for each mooring from the local bathymetry based on the GEBCO_2014 bathymetry grid (The GEBCO_2014 Grid, version 20150318, `http://www.gebco.net`) and using an average length scale of the order of 10 km. The estimated accuracy of $\beta$ is approximately $\pm 10°$."

Figure 4. An alternative way of including the rotational properties of the velocity series

could be to plot them as rotational ellipses (major and minor axis), together with as already done different colors for CW and ACW.
Reply: Thanks for the suggestion, we are aware of this possibility. In Fig. 4 (now 5), we show the orientation of the major axis and the rotation of the current, but want to show the spatial distribution of the maximum tidal KE as well, which is done easiest using circles scaled to the amount of tidal KE.

Line 167: In most instances the authors use "austral " winter/summer. Not always . For clarity be sure that this is consistent through the ms.
Reply: We agree, this should be done consistently throughout the manuscript. We have now included "austral" everywhere where it might be ambiguous.

Line 186-187: "The bathymetry represents an average of six across-slope sections in the area of moorings M1 to M5". I understand that it is necessary to make some representative bathymetry, but some more details and motivation would be good.
Reply: We used the same bathymetry as Jensen et al. (2013) after having compared it to our larger study area. The paragraph has been rephrased to explain this more clearly: "Following Jensen et al. (2013), we use a closed coastal but open offshore boundary, a free surface and a negligible bottom friction. Furthermore, we apply the same bathymetry as Jensen et al. (2013). It represents an average of six across-slope sections with approximately 20 km separation in the area of moorings M1 to M5 and compares well to sections farther west in our study area (not shown)."

Line 199. What is meant by the M-mooring array?
Reply: The M-mooring array comprises moorings M1 to M5. We changed the sentence to avoid possible confusion: "Figure 8a shows the obtained density and stratification profiles, representative for the shelf break at moorings M1 to M5 in austral summer."

Figure 8. Legend is not easy to read. In particular I have problem with what is meant by the "ref top" and ref 80. Please clarify this.
Reply: We changed the legend (and the figure caption). The legend includes now "bathy east", a run based on the reference stratification with the steeper bathymetry east of the study area, and "surface top" and "surface mean". These are runs for the reference stratification with a differently inferred surface $N^2$ value, as the uppermost stratification value in the numerical code covers the upper 160 m. The run "surface top" uses the uppermost value of the observational stratification profile for the stratification in the code, and the

run "surface mean" uses the average of the upper 80 m of the observed stratification profile.

Line 247: Maybe change to ".. a 40 km wide current with a westward core velocity of 0.2 m s-1 and . . . ".
Reply: Thanks for your suggestion, which we followed. The sentence reads now more easily.

Line 263: Change "to coincide with a tidal" to "to coincide with one exact tidal .."
Reply: We changed the sentence according to your suggestion.

Fig 5. This figure must be improved and better simplified.
Reply: See comments from the other two reviewers. We removed the previous Fig. 5b and explained the contents of panel a) better, with the help of a new panel b).

Line 356-358: Somewhat unclear what is meant here. Do you suggest that the semi-diurnal tide is what sets the stratification that provide the conditions for DTW, or is the point that semi-diurnal is major cause for mixing at the shelf break. Since this point is already mentioned in the introduction a possibility is simply to delete it here.
Reply: The latter is what we mean; the semi-diurnal tide is the major cause for mixing at the shelf break. We rewrote the paragraph and changed also the sentence you refer to: "In addition, the tides in the area will greatly influence mixing (Fer et al., 2016) and hence modify the stratification in the shelf break area.

## Revised manuscript

Manuscript prepared for Ocean Sci.
with version 2015/09/17 7.94 Copernicus papers of the LaTeX class copernicus.cls.
Date: 5 October 2016

# Seasonal resonance of diurnal coastal trapped waves in the southern Weddell Sea, Antarctica

Stefanie Semper[1] and Elin Darelius[1,2]

[1]Geophysical Institute, University of Bergen, and Bjerknes Centre for Climate Research, Bergen, Norway
[2]Uni Research Climate, Bergen, Norway

*Correspondence to:* stefanie.semper@uib.no

**Abstract.**

The summer enhancement of diurnal tidal currents at the shelf break in the southern Weddell Sea is studied using velocity measurements from 29 moorings during the period 1968 to 2014. Kinetic energy associated with diurnal tidal frequencies is largest at the shelf break and decreases rapidly with distance from it. The diurnal tidal energy increases from austral winter to summer by, on average, 50 %. The austral summer enhancement is observed in all deployments. The observations are compared to results from an idealised numerical solution of the properties of coastal trapped waves (CTWs) for a given bathymetry, stratification and an along-slope current. The frequency at which the dispersion curve for mode 1 CTWs displays a maximum (i.e. where the group velocity is zero and resonance is possible) is found within or near the diurnal frequency band, and it is sensitive to the stratification in the upper part of the water column and to the background current. The maximum of the dispersion curve is shifted towards higher frequencies, above the diurnal band, for weak stratification and a strong background current (i.e. austral winter-like conditions) and towards lower frequencies for strong upper layer stratification and a weak background current (austral summer). The seasonal evolution of hydrography and currents in the region is inferred from available mooring data and conductivity-temperature-depth profiles. Near-resonance of diurnal tidal CTWs during austral summer can explain the observed seasonality in tidal currents.

## 1 Introduction

The shelf break region in the southern Weddell Sea (Fig. 1) is an area of great climatic interest. This is where cold and dense water masses, formed on the continental shelf and underneath the Filchner-Ronne Ice Shelf (FRIS), cross the shelf break and descend the continental slope (Foster and Carmack, 1976; Foldvik et al., 2004; Nicholls et al., 2009), ultimately contributing to the formation of Antarctic Bottom Water which spreads out into the major oceans at abyssal depths (Orsi et al., 1999). Furthermore, warm off-shelf water, referred to as Modified Warm Deep Water (MWDW), crosses the shelf break during austral summer (Årthun et al., 2012), flows southward towards the

Filchner Ice Shelf along the eastern flank of the Filchner Depression (Foldvik et al., 1985a, see map in Fig. 1 for location) and reaches, at least occasionally, the Filchner Ice Shelf front during austral autumn (Darelius et al., 2016). Climate models suggest a larger inflow and a dramatic increase in basal melt rates below the FRIS within the next century (Hellmer et al., 2012).

Physical processes at the shelf break and on the continental slope influence both the cold outflow and the warm inflow in terms of their hydrographic properties and strengths. The variable depth of the thermocline, for example, which is controlled mainly by wind forcing and eddy overturning (Sverdrup, 1953; Nøst et al., 2011) will determine if and when warm water can access the continental shelf (Årthun et al., 2012). Meanwhile, variability in off-shelf water properties will alter the density contrast between the cold outflow and the ambient water, and thus the strength of the geostrophically balanced outflow (Kida, 2011; Wang et al., 2012). It will also influence the properties of the descending dense plume, since it is a mixture of outflow water and ambient water (Darelius et al., 2014). The co-location of the critical latitude for the tidal component $M_2$ and a critical slope leads to enhanced turbulence levels in the region (Fer et al., 2016). Mixing can be expected to be further enhanced at the shelf break by the strong diurnal tidal currents (Fer et al., 2015; Pereira et al., 2002). The strong diurnal tidal currents in the study region have been linked to the presence of continental shelf waves (Foldvik and Kvinge, 1974; Middleton et al., 1987; Foldvik et al., 1990), a class of coastal trapped waves (CTWs). Tidally generated CTWs at diurnal frequencies in the shelf break region of the southern Weddell Sea are also the focus of this study.

CTWs can be generated by e.g. tides (Thomson and Crawford, 1982) or wind (Huthnance, 1995). Additionally, a connection between the generation of the waves and the outflow of dense shelf water through troughs has been suggested (Marques et al., 2014; Jensen et al., 2013). CTWs with subinertial frequencies propagate along a trapping boundary, e.g. a coastal wall or a sloping bottom (Huthnance, 1995; Huthnance et al., 1986). The waves require the support of such a boundary to exist and decay exponentially with increasing distance from it (Mysak, 1980). While CTWs propagate with shallow water to the left (in the southern hemisphere), the group velocity $c_g$, and thus the energy associated with the waves, can propagate in either direction (Fig. 2). If the group velocity is zero, i.e. for a maximum in the dispersion curve of a wave, energy cannot propagate. When the frequency of this maximum (hereafter called "resonant frequency", RF) in the dispersion relation coincides with the frequency of tidal currents, resonance may occur and tidal currents will be amplified. In practice, energy likely escapes in one or the other direction along the slope. Leakage of energy occurs for example because of irregularities in the bathymetry and because the bottom slope changes (i.e. isobaths converge or diverge, Thomson and Crawford, 1982). Therefore, we use the term near-resonance rather than resonance.

Such near-resonant diurnal CTWs were first recorded on the shelf of the Outer Hebrides of Scotland by Cartwright (1969) and have been observed and modelled at numerous occasions and locations since then (e.g. Huthnance, 1974; Crawford and Thomson, 1982; Heath, 1983; Hunkins, 1986;

Padman et al., 1992; Skarðhamar et al., 2015). In our study region, Foldvik and Kvinge (1974) and Foldvik et al. (1985b) first suggested that CTWs caused the observed strong diurnal tidal currents, which broke down during austral winter presumably due to a seasonally varying stratification. Later, Middleton et al. (1987) and Foldvik et al. (1990) found a particularly strong enhancement of the $K_1$ tidal constituent during austral summer. The summer maximum was hypothesised to be due to the interaction of barotropic CTWs with topography in the presence of a seasonally variable mean current (Foldvik et al., 1990). These studies were based on a small number of moorings and a barotropic shelf wave model neglecting the effects of stratification.

Our study is based on a more extensive data set as observations of current velocities from 29 moorings are used to quantify the strength of diurnal tidal currents and to describe their spatial and temporal variability. We provide a novel description of the seasonal changes in shelf break hydrography based on observations, and use a numerical code (Brink, 2006) to investigate the sensitivity of the CTW properties to seasonal changes in hydrography. Seasonally varying hydrography and currents are known to alter the properties of the CTWs (e.g. Marques et al., 2014; Jensen et al., 2013; Brink, 1991; Wang and Mooers, 1976). Foldvik et al. (1990) showed how changes in the background current will affect the phase of diurnal CTWs, which are assumed to be generated upstream, as they arrive in the study region. Here we investigate, similar to the work by Skarðhamar et al. (2015), the effect of changes in the background current on the dispersion relation and hence on the possibility for local near-resonance. We hypothesise that the observed seasonality in the diurnal tidal currents is indirectly linked to seasonal changes in the oceanographic "background", as it determines the dispersion relation including the RF for the CTWs which are responsible for the tidal amplification in the area.

Another seasonal phenomenon which can potentially influence the CTW generation is sea ice. Frictional damping of tidal CTWs due to sea ice is suggested to be the cause of the observed reduction of tidal currents over the shelf in the Sea of Okhotsk during winter when the sea ice cover exceeds 80% (Ono et al., 2008). Strong tidal currents in turn are important for local sea ice deformation (Padman et al., 1992) and hence sea ice concentration (Mack et al., 2013). A study by Nakayama et al. (2012) showed that CTWs can locally enhance sea ice drift. Here, we study the seasonal variability of sea ice cover in the southern Weddell Sea and discuss its potential relevance for CTWs.

Finally, we investigate the role of divergent bathymetry; the continental slope steepens considerably to the east of our study region (Fig. 1) and isobaths hence diverge in the direction of CTW propagation. Numerical simulations from the Barents Sea region showed that tidally generated CTWs were confined to a region of divergent bathymetry (Skarðhamar et al., 2015).

Discussing the effects of seasonal varying hydrography and currents, sea ice and bathymetry, this article aims to provide new insight into the seasonal variability of the tidal currents at diurnal frequencies and its causes in the southern Weddell Sea.

## 2 Data and methods

Current meter data from 29 moorings (Foldvik et al., 2004; Jensen et al., 2013; Darelius et al., 2016) located on the continental slope and shelf in the area surrounding the Filchner Depression have been analysed. The records span the years 1968 to 2014 and are of 1–2 years duration. The locations of the moorings are shown in Fig. 1, and deployment details are listed in Table 1. The mean currents included in Fig 1 are vertical means for moorings M1 to M5, while for moorings C, W2, W3, F3 and F4 only the uppermost instrument has been considered to minimise the effects of the Ice Shelf Water plume. Temperature records suggest that plume water is rarely present at these levels.

The coordinate system is rotated clockwise to align the $y$-axis with the isobaths, agreeing with the set-up of the numerical code (Brink, 2006) in the southern hemisphere. $u$ is thus directed on-shelf and $v$ along the continental slope (Fig. 1). The rotation angle $\beta$, positive for clockwise rotation, is listed in Table 1; it is inferred for each mooring from the local bathymetry based on the GEBCO_2014 bathymetry grid (The GEBCO_2014 Grid, version 20150318, http://www.gebco.net) and using an average length scale of the order of 10 km. The estimated accuracy of $\beta$ is approximately $\pm 10^{\circ}$.

Time series of kinetic energy (KE) associated with the diurnal tidal currents are constructed as follows: The hourly-averaged current meter data are divided into intervals of 1.5 months length beginning every 14th day. For each interval, the power spectral densities are estimated using Welch's method (Welch, 1976) and 14 day long, 50 %-overlapping Hanning windows. The diurnal tidal KE is obtained by integrating the velocity spectra,

$$\mathrm{KE} = \int_{\omega_1}^{\omega_2} (S_u + S_v)\, d\omega, \tag{1}$$

where, following Jensen et al. (2013), $\omega_1$ and $\omega_2$ correspond to periods of 26.9 h and 21.3 h respectively.

Diurnal tidal KE has also been inferred using tidal predictions from the Circum-Antarctic Tidal Simulation version 2008b (CATS2008b), an updated version of the linear tidal inverse model described by Padman et al. (2002). The barotropic currents at the specific tidal frequencies are predicted for the respective time and location of every mooring deployment and are treated in the same way as the observational current velocities.

Tidal ellipses, i.e. major and minor axes, inclinations and Greenwich phases, have been obtained from the mooring records using harmonic analysis (T_TIDE, Pawlowicz et al., 2002), a Matlab version of the FORTRAN code developed by Foreman (1978).

Records of temperature and salinity from mooring M3, located at the 725 m isobath just east of the Filchner Depression sill (Fig. 1), are used to describe the seasonal changes in hydrography at the shelf break and upper continental slope. The mooring records are complemented by a conductivity-temperature-depth (CTD) profile obtained during the deployment cruise in 2009 and by hydrographic measurements obtained in the vicinity of the M3 location (within 10 km, Fig. 1) provided by seals

tagged with small CTD sensors (described in Århun et al., 2012, hereafter referred to as "seal data"). The accuracies of the seals' temperature and salinity measurements are stated to be 0.005° C and 0.02, respectively (Boehme et al., 2009).

In addition, we use wind observations from Halley Research Station, located at 75° 35' S, 26° 39' W (Fig. 1), from 1957 to 2014 (British Antarctic Survey, 2013, updated 2014) and satellite derived records of sea ice concentration (Meier et al., 2013, updated 2015), available for the period 1978 to 2014. The sea ice concentration is averaged over the study area (inset in Fig. 1).

## 3 Observational results

### 3.1 Spatial and temporal variability of tidal currents

The diurnal tidal frequency band shows enhanced variance for both the $u$- and $v$-component, especially at the frequencies of the most important diurnal tidal constituents $K_1$ and $O_1$ (Fig. 3). High energy levels are additionally observed at semi-diurnal frequencies and around 35 h, as also found by Jensen et al. (2013) and Darelius et al. (2009).

The energy associated with the diurnal tidal currents, the diurnal tidal KE (Sect. 2), shows little variation with depth, except at the lowest measurement level at 25 m.a.b. In this bottom boundary layer, the diurnal tidal KE is slightly decreased compared to the overlying water column (Fig. 4). Depth-averaged diurnal tidal KE is used for further analysis.

Figure 5 shows the spatial distribution of diurnal tidal KE during austral summer. The magnitude of diurnal tidal KE is highest directly at the shelf break (e.g. moorings B2, F1, M3) and decreases rapidly with distance from it. The tidal currents rotate clockwise on the deeper continental slope and anticlockwise at the shelf break and on the shelf. The major axes of the tidal ellipses at the $K_1$ frequency are directed across the continental slope for moorings located at the shelf break and on the continental slope (especially for the ones east of the Filchner Depression and west of the ridge). Hence, the diurnal tidal energy is higher in the across-slope component than in the along-slope component. Tidal currents recorded at moorings on the shelf are close to circular.

Time series of diurnal tidal KE (Fig. 6a) show two local maxima; one in austral summer and one in austral winter. The austral summer maximum is 30 % to 180 % higher than the winter maximum. This amplitude difference is especially strong in records from moorings on the continental slope and at the shelf break, but it is observed in all deployments of sufficient length. For moorings on the continental shelf, the difference between the maxima is sometimes less pronounced (e.g. Fr2 in Fig. 6a). Tidal KE inferred from the tidal model CATS (Fig. 6b) shows two annual peaks of similar amplitude. The two peaks are the result of $K_1$–$P_1$ interference (see Sect. 5), but astronomical forcing cannot explain the observed difference in tidal KE between austral summer and winter.

Estimates of wavelengths were obtained from mooring pairs M1–M4 and M2–M5, based on the difference in Greenwich phase obtained from T_TIDE. The mooring pairs were deployed roughly

along the 1100 m and 1950 m isobaths at a distance of 71 km and 86 km, respectively. For the $O_1$ tidal constituent, the uncertainty and hence the range is large during austral summer (200 km–1600 km), while austral winter values are found in the range 300 km–600 km. The wavelength obtained for $K_1$ is in the range 250 km–500 km for all seasons.

### 3.2 Seasonal variability of the hydrography and current on the upper slope

The seasonal variability in the hydrography at the shelf break and on the upper slope is investigated by merging all available observational data (moorings, CTD, seal data) near the location of mooring M3 (Fig. 7a,b). Cold and fresh Winter Water (WW) is found on top of warm and saline MWDW. MWDW is a mixture of WW and Warm Deep Water (WDW), the Weddell Sea version of the Circumpolar Deep Water which composes most part of the Antarctic Circumpolar Current.

While the temperature in the upper approximately 400 m is near the freezing point year-round, the salinity of the surface layer increases from 34.0 in February to 34.4 in October. The cold and fresh surface layer during austral summer likely results from local sea ice melt.

The thermocline is found at a depth of approximately 400 m from December to April and deepens by 200 m to approximately 600 m during May to August. The deeper moorings (e.g. M5) show that seasonal changes in the water column below the thermocline are negligible (not shown). Generally, the seal data show higher salinities and temperatures at depth compared to the mooring data (also compared to the range of the unfiltered mooring records, not shown), suggesting that the MWDW and the thermocline are found higher up in the water column in 2011 compared to 2009.

The density profiles (Fig. 7c) show a gradual increase in density at the surface from $\sigma_0 \approx 27.3\,\mathrm{kg\,m^{-3}}$ to $27.7\,\mathrm{kg\,m^{-3}}$, indicating a relatively stable stratification in the upper part of the water column during austral summer and a relatively homogeneous, weakly stratified upper layer during austral winter.

Observations of the Antarctic slope current flowing westward along the shelf break in the Weddell Sea are relatively scarce, and our knowledge of its strength, width and variability in our study region are limited. Upstream, at 12° W, Fahrbach et al. (1992) observed a south-westward flowing current following the continental shelf break with annual mean velocities of $10\,\mathrm{cm\,s^{-1}}$–$20\,\mathrm{cm\,s^{-1}}$ and a maximum velocity (hourly average) of over $60\,\mathrm{cm\,s^{-1}}$. Although inconclusive, the records suggest a wind-driven seasonal cycle with a magnitude of about $5\,\mathrm{cm\,s^{-1}}$ where maximum currents are observed in late austral autumn.

At 17° W, the core of the slope current is found above the 1000 m isobath with a westward surface velocity of $50\,\mathrm{cm\,s^{-1}}$ (Heywood et al., 1998). The current is suggested to weaken towards Halley Bay (Fahrbach et al., 1992), and at 27° W, it splits into two branches, where one branch follows the coast southwards and the other one continues along the continental slope (Gill, 1973) into our study region.

Mooring records from the region west of the Filchner Depression cover mainly the lower part of the water column, and the majority of the observations are greatly influenced by the Filchner

overflow plume (Foldvik et al., 2004), thus giving little information about the slope current. Fig. 1 shows annual mean currents from moorings and instrument levels in the area, that, based on the accompanying temperature records, are not directly affected by the dense outflow of Ice Shelf Water (Sect. 2).

East of the depression, the strongest along-slope currents are observed at mooring M3, relatively close to the shelf break at the 750 m isobath. Here, the magnitude of the annual mean current is 10 cm $s^{-1}$–17 cm $s^{-1}$ (directed westward and stronger towards the bottom) while monthly mean values reach 25 cm $s^{-1}$ during austral winter.

At mooring M4 (located at the 1050 m isobath, less than 10 km north of M3, Fig. 1), a much weaker westward (3 cm $s^{-1}$) mean current was observed, and austral winter values reached 8 cm $s^{-1}$. At M5 (1976 m depth, about 40 km north of M3), the magnitude of the annual mean current is $<$1 cm $s^{-1}$ with a peak in early austral winter of 2-3 cm $s^{-1}$.

The limited observations available from our study region suggest a westward flowing jet, which is relatively narrow and appears to be centred at the shelf break. The jet intensifies and widens during early austral winter. Winter time intensification of the slope current is also observed by Núñez-Riboni and Fahrbach (2009) and Graham et al. (2013).

## 4 Numerical code

### 4.1 Set-up

The numerical code described in Brink (2006) and adapted for the southern hemisphere by Jensen et al. (2013), is used to calculate the properties of stable, inviscid CTWs for different stratification, bathymetry and mean flow.

The code was set up using 30 vertical levels and 120 horizontal grid points to represent a 2 D-cross-slope section. This is within the recommended range of grid points; increasing the resolution leads to instability and failure of the test for hydrostatic consistency. Following Jensen et al. (2013), we use a closed coastal but open offshore boundary, a free surface and a negligible bottom friction. Furthermore, we apply the same bathymetry as Jensen et al. (2013). It represents an average of six across-slope sections with approximately 20 km separation in the area of moorings M1 to M5 and compares well to sections farther west in our study area (not shown).

The input stratification vector (squared buoyancy frequency, $N^2$) is linearly interpolated onto the vertical levels of the code and duplicated for the horizontal cross-shelf section before it is converted to density, hence no across-shelf stratification changes are taken into account. If an along-shore current is specified, the background density field is altered by applying the thermal wind equation. The stratification at each level $n$ is then determined from the density difference between levels $n-1$ and $n+1$.

### 4.2 Sensitivity to stratification

A reference stratification profile was constructed based on all available CTD data collected in January and February in the eastern part of the study area. Similar profiles were constructed for areas farther to the west. Figure 8a shows the obtained density and stratification profiles, representative for the shelf break at moorings M1 to M5 in austral summer. A simplified version of the stratification profile (Fig. 8b) indicates the parameters changed in the sensitivity test: the strengths of the surface magnitude (SM) and the subsurface magnitude (SSM) around 500 m depth, the depth of the SSM (SSD) and the constant magnitude at depths below 1200 m ("deep magnitude", DM). The values of the applied parameter values are listed in Table 2.

The dispersion curves and their group velocities for wave modes 1 to 3 corresponding to the reference stratification (Fig. 8a) are presented in Fig. 9. Mode 1 is the only wave mode for which the dispersion curve shows a maximum, i.e. where the group velocity becomes zero. These results suggest that CTWs with a wavelength of approximately 1260 km and a period of approximately 30 h will be trapped while CTWs with tidal frequencies cannot exist. For tidal CTWs to exist, the dispersion curve must pass through the tidal band, i.e. the maximum of the dispersion curve (the resonant frequency, or "RF") must lie within (thus giving near-resonance) or above the diurnal tidal frequency band.

As the numerical code has a vertical resolution of 160 m, defining the uppermost $N^2$ value, which ought to represent the considerable changes close to the surface, is not a straightforward task. For the reference stratification profile (Fig. 8), the surface $N^2$ value used in the numerical code is from 20 m depth. Using the surface profile value ("surface top" in Fig. 9) or an average of the upper 80 m ("surface mean" in Fig. 9) shifts the dispersion curve and thus the RF to higher frequencies (Fig. 9). For stratification profiles which are representative for areas farther west at the shelf break and constructed similarly to the reference stratification with surface $N^2$ values of the upper 80 m average ("stratification 2–4"), the dispersion curve and RF are similarly shifted to higher frequencies (Fig. 9).

Keeping in mind the variations along the shelf break and with different approaches on how to choose the uppermost stratification value, the characteristic parameters of the reference profile (SM, SSM, SSD, DM, Fig. 8b) are varied in the following to explore the general effects of stratification on the dispersion curve and the RF.

Figure 10 shows the results from the sensitivity test for stratification, where the RF is identified from each dispersion curve obtained from the modified stratification input. An increase of $N^2$ at the surface (case SM) leads to a decrease in RF, which moves through the diurnal tidal frequency band for the modelled range of surface stratification. Contrarily to case SM, an increase of the stratification maximum at approximately 640 m depth (case SSM) increases the RF. The effect of an increase in depth of the subsurface maximum (case SSD) results in an apparent decrease of the RF. However, due to the interpolation in the numerical code, the stratification around the subsurface maximum as

well as the exact value of the maximum are difficult to preserve. Hence, the actual effect of case SSD appears to be rather small. Varying the stratification below 1200 m depth (case DM) has a negligible effect on the RF.

### 4.3 Sensitivity to along-slope current

The optional along-shore current in the numerical code has a Gaussian shape; its offshore, onshore, upward and downward $e$-folding length scales must be specified, in addition to the centre position, strength and depth of the current.

For the sensitivity test, a barotropic (i.e. with a large vertical length scale) westward current is assumed which is centred at the shelf break. The density is set to be undisturbed at the coast when the density field is altered according to the thermal wind equation, with the input $N^2$ vector being the reference stratification for all runs. The width and strength of the current are varied from 10 km to 100 km and magnitudes of 0.1 m s$^{-1}$ to 0.5 m s$^{-1}$, respectively (Fig. 11). This roughly encompasses the observed structure and variability of the slope current described in Sect. 3. Generally, both a stronger and a wider current lead to an increase in RF; with the effect of increased current strength being largest.

In another test, the location of the current core was moved 40 km on and off shore relative to the shelf break. The sensitivity of the RF decreases slightly when the current core is located off shore from the shelf. The magnitude of the change in RF for a 40 km off-shore shift depends on the width of the current, but it is comparable to a change in current velocity of $\pm 10$ cm s$^{-1}$ (Fig. 11).

Although the overall effect of an added barotropic slope current is minor compared to the sensitivity to changes in stratification (cf. $y$-axes in Fig. 10 and Fig. 11), the sensitivity depends noticeably on the vertical length scale. As an example, a 40 km wide current with a westward core velocity of 0.2 m s$^{-1}$ and a reduced downward $e$-folding length scale (2000 m instead of 4300 m) is chosen. The RF is then considerably larger (open circle in Fig. 11) than for the more barotropic case.

## 5 Discussion

Observations from the continental slope in the southern Weddell Sea show anomalously strong tidal currents at diurnal frequencies (Middleton et al., 1987). Our extended analysis – including all current meter records (1968–2014) from the region – confirms previous findings suggesting that the strong currents are the result of tidally forced CTWs (Middleton et al., 1987; Foldvik et al., 1990, 1985b).

The observations agree qualitatively with the mode 1 CTW "generated" in the numerical code provided by Brink (2006). As expected, the rotational direction of the observed and simulated currents changes from anticlockwise on the upper part of the continental slope to clockwise on the deeper part of the slope, and the strength of the diurnal tidal currents increases towards the shelf break (Fig. 12).

The wavelengths inferred from the observations are generally consistent with those obtained from the numerical code for cases where CTWs of diurnal frequencies are allowed.

Time series of the KE associated with the diurnal tides show a persistent pattern with two annual peaks, one in austral summer and one in austral winter, and minima near the equinoxes in spring and autumn, when both the sun and the moon are close to the equator. The austral summer peak is consistently enhanced by 30 % to 180 % compared to the austral winter peak.

The semi-annual signal, i.e. the two peaks, is likely the result of interference between the diurnal tidal constituents $K_1$ and $P_1$ which are in phase every six months. At e.g. the location of moorings M3 and M5, the $P_1$ amplitude predicted by the tidal model CATS is about 1/2 of the $K_1$ amplitude, and the combined amplitude hence varies from 0.5 to 1.5, i.e. with a factor of three, over a period of six months. This results in two semi-annual peaks with similar amplitude (Fig. 6b). The observed difference between peak and minimum values are in rough agreement, although on the high end when compared to CATS2008b. Astronomical forcing can however not explain the asymmetry between the two peaks, i.e. the observed austral summer enhancement of the diurnal tidal energy.

It is possible that other factors contribute to the observed semi-annual variability, such as e.g. a semi-annual cycle of mixing (and hence stratification) caused by the $K_1$–$P_1$ interference, or a superposition of two annual cycles (e.g. stratification and background current) affecting the diurnal KE with an offset in time (L. Padman, personal communication, 9 August 2016).

We hypothesise that the enhancement of tidal KE during austral summer is caused by near-resonance of diurnal CTWs. The obtained dispersion relations suggests that diurnal CTWs may be near-resonant, i.e. that the group velocity is zero or close to zero at diurnal frequencies so that energy cannot propagate out of the area, which results in amplified diurnal tidal currents. Near-resonance of diurnal CTWs in the study region was also suggested by Middleton et al. (1987) using a barotropic shelf wave model (Saint-Guily, 1976). The dispersion relation is shown to be relatively sensitive to changes in the upper ocean stratification, and the observed seasonal changes in upper ocean hydrography discussed below causes the RF to move through the diurnal tidal band, so that diurnal CTWs are "nearer" resonance during austral summer than during austral winter, when the RF falls above the diurnal band. Tidal currents may be enhanced for a range of frequencies surrounding the RF, and thus the RF does not need to coincide with one exact tidal frequency for amplification to occur (Chapman, 1989).

The largest seasonal changes in the shelf break hydrography in the region occur, similar to regions farther east in the Weddell Sea (Nøst et al., 2011; Graham et al., 2013), above the pycnocline. Cooling and a gradual increase in salinity (due to ice freezing and brine rejection) during austral autumn and winter leads to a gradual deepening of the surface layer. Towards the end of the winter (August–September) the upper 400 m are relatively homogeneous. During austral summer, the winter layer is capped by a fresh and relatively warm surface layer which likely is the result of local sea-ice melt and solar heating. The layer of summer surface water is thin (10 m–100 m, see CTD-profile in Fig. 7)

and greatly increases the stratification by creating a seasonal, shallow pycnocline. The sensitivity test (Fig. 10) shows that the value of the RF is sensitive to the stratification in the upper layer (SM) and that it increases for decreasing stratification. The response in RF to realistic changes in SM is of sufficient magnitude to cause the RF to move through the diurnal tidal band.

While the RF is influenced by changes in the strength of the permanent (deeper) pycnocline (SSM), which is the manifestation of the transition from WW above to MWDW and WDW below, there is no observational evidence suggesting that it would change in magnitude. The depth of the permanent pycnocline (SSD), however, increases from about 400 m in austral summer to about 600 m, but changes in SSD have little or no influence on the RF.

Despite the fact that the stratification affects the dispersion curve of CTWs considerably (Fig. 9), CTWs are relatively barotropic in the region (Fig. 4 and Fig. 12; Middleton et al., 1987; Jensen et al., 2013). This is expected since the Burger number is $Bu = \left(\frac{NH}{fL}\right)^2 \approx \mathcal{O}(10^{-4}) \ll 1$, where $N^2$ is the stratification ($N$ =(0.97–1.7)·$10^{-3}$ $s^{-1}$), $f$ the Coriolis factor (-1.4·$10^{-4}$ $s^{-1}$) and where $H$ (400–600 m) and $L$ (300.000–500.000 m) are representative depth and length scales, respectively.

Foldvik et al. (1990) suggested that the observed seasonality was linked to the variability of the slope current. The available observations of the slope current are limited and do not allow a detailed description, but the data from moorings M1 to M5 suggest, in agreement with observations upstream (Nøst et al., 2011; Graham et al., 2013; Núñez-Riboni and Fahrbach, 2009), that the westward flowing slope current is intensified during austral winter. When a barotropic, westward background current is included in our numerical set-up, the dispersion curve (and thus the RF) is shifted toward higher frequencies (Fig. 11 and Jensen et al., 2013), but the effect is small compared to the effect of stratification changes. The stronger current observed during austral autumn and winter will however add to the effect of the low winter time stratification and move the RF to higher frequencies.

The low values of tidal KE during austral winter can potentially be caused by frictional damping of CTWs by sea ice. While tidal energy cannot be dissipated when ice is drifting freely, high ice concentration provides the friction which is needed to reduce tides (Padman et al., 2002). This mechanism was suggested by Ono et al. (2008) to explain the reduction in tidal CTW energy observed at at one of their mooring sites during winter. The reduction was only observed at the site away from the region of CTW generation, indicating the cumulative effect of frictional dampening over distance. However, the authors fail to explain why the period with reduced tides are much shorter (and misaligned) compared to the period with dense (>80 %) sea ice cover.

The ice cover in the study region normally exceeds 90 % during austral winter (mid-April to mid-November) and decreases to a minimum of on average 50 % in February (Fig. 14), and high (low) sea ice concentration hence coincides with low (high) diurnal tidal energy levels, as expected if frictional damping by sea ice is important. The semi-diurnal tidal currents, however, are observed to be larger during austral winter than during summer (Foldvik et al., 1990), rendering a considerable

effect of sea ice questionable. We can unfortunately neither quantify nor rule out the relevance of sea ice concentration and sea ice dampening to the observed seasonality of the diurnal tidal currents.

While the tidal force is the main generation mechanism for CTWs in the diurnal tidal band (Thomson and Crawford, 1982), CTWs can also be generated by wind (Huthnance et al., 1986). Short duration storms have been observed to excite near-resonant CTWs of mode 1 (Gordon and Huthnance, 1987), i.e. the response to storms would in our case resemble the tidally forced waves. Time series of wind from the nearby Halley Research Station (see Fig. 1 for location), however, show that storms (wind speed $>20\,\mathrm{m\,s^{-1}}$) are rare during austral summer and, as expected, more frequent during winter and early spring. CTWs induced by storms can hence not explain the summer enhancement of the diurnal tidal currents. Fourier analysis of the time series reveals a daily cycle in wind strength with an increase of magnitude of up to $1.4\,\mathrm{m\,s^{-1}}$ around noon, which likely results from local boundary layer effects: The stable boundary layer which develops during the night is destroyed during the day by mixing due to solar insolation (see, e.g. Stull, 2012). Since the signal is weak, we conclude that these oscillations are not responsible for the observed summer amplification.

The CTWs owe their existence to topography, and the dispersion curve is sensitive to changes in bathymetry (e.g. Jensen et al., 2013, and Fig. 9). Just east of our study region, the continental slope is much steeper (Fig. 1), i.e. the isobaths diverge towards the west. Divergent bathymetry has been shown to allow for the generation of diurnal CTWs (Skarðhamar et al., 2015). On a divergent slope, tidal energy travelling along the slope may slow down and converge as the group velocity decreases due to the changing topography, while energy travelling in the other direction will speed up and diverge. There are no direct observations of tidal currents from the steep, eastern region, but the tidal motion of sea ice above the shelf break there suggests weaker currents compared to the study region (Padman and Kottmeier, 2000). The wavelengths of the diurnal CTWs are typically large compared e.g. to the length scale over which the changes in bathymetry discussed above occur and the scale of other topographic features in the area. While the implications of this are beyond the scope of the current study, we note that the CTWs modelled by Skarðhamar et al. (2015) similarly have wavelengths which are considerably larger than the topographic scales. A full 3 D-analysis, similar to the one by Skarðhamar et al. (2015), would be needed to fully explore the effect of bathymetry on CTWs in the study region.

The anomalously large diurnal tidal currents and the CTWs will potentially influence the exchange of WDW across the shelf break. In an idealised model study, CTWs were shown to enhance the inflow of warm water through a trough cross-cutting the continental shelf (St-Laurent et al., 2013), similar to the Filchner Depression. We note that the depth of the WW–WDW transition (identified e.g. by the -1° C isotherm) varies on diurnal time scales (Fig. 13a), and e.g. in December 2009, the vertical excursion of the isotherm associated with the diurnal tides is $>100\,\mathrm{m}$ (Fig. 13b). The depth of the transition is likewise affected by CTWs with 35 h period (Fig. 13; Jensen et al., 2013). The existence and strength of diurnal (and longer period, Jensen et al., 2013) CTWs in the region must

hence be expected to directly influence the availability of warm water above the shelf depth, i.e. at depths where it can potentially access the continental shelf through the influence of other processes such as e.g. a background mean flow, rectified tidal flows, friction or eddy exchanges. In addition, the tides in the area will greatly influence mixing (Fer et al., 2016) and hence modify the stratification in the shelf break area. Modelling efforts aiming to describe and predict the oceanic heat transport towards the FRIS cavity thus ought to include tidal forcing to correctly capture the dynamics at the shelf break.

Finally, we mention that the observed diurnal tidal currents are up to one order of magnitude larger than those predicted by the tidal model CATS2008b (Fig. 12, Padman et al., 2002), which does not include stratification or the variability of mean circulation required to predict seasonal modulation of tidal currents. Moreover, due to discrepancies in the model bathymetry, the predicted peak tidal currents are not consistently aligned with the shelf break when running CATS along a cross-shelf section through the locations of moorings M1 and M2 (see Fig. 12 and Fig. 1 for location of section). Hence, care must be taken when using CATS to de-tide velocity observations from the study region.

## 6 Conclusions

Velocity measurements at 29 moorings located on the continental slope and shelf in the southern Weddell Sea from the period 1968 to 2014 show pronounced diurnal tidal variability. Diurnal tidal currents are strongest at the shelf break and substantially enhanced during austral summer. The summer enhancement is not predicted by the tidal model CATS2008b (Padman et al., 2002), as the model does not include stratification or the variability of mean circulation. We investigated the possibility for near-resonant CTWs causing the enhanced diurnal tidal currents by using a 2 D-numerical code to obtain CTW properties (Brink, 2006). Dispersion curves of mode 1 CTWs have a maximum in frequency (the resonant frequency, or "RF"), which results in zero group velocity, i.e. trapped energy. The RF moves in and out of the diurnal tidal frequency band depending on the stratification and the slope current which both vary seasonally as hydrographic and current observations at the shelf break reveal. For the weakly stratified water column and strong slope current during austral winter, the RF is found above the diurnal band, suggesting the generation of weak, non-resonant tidal CTWs which quickly propagate out of the generation area. For austral summer conditions, i.e. a more stratified upper water column combined with a weaker slope current, the RF can fall into the diurnal band, thus leading to near-resonant diurnal CTWs enhancing the tidal currents.

While no direct influence of wind on the diurnal tidal currents and no evidence of sea ice affecting the diurnal CTWs have been found, the varying bathymetry east of the study area likely affects the propagation of the CTWs. Further studies, using 3 D-models for example, are needed to quantify these influences as well as to detect the generation site of the CTWs.

The shelf break region in the southern Weddell Sea is an area of great climatic interest. Cold, dense water descends the continental slope and contributes eventually to the formation of Antarctic Bottom Water, while warm MWDW flowing onto the shelf prospectively may reach the cavity below FRIS, thus enhancing basal melt rates. The strong diurnal tidal currents at the shelf break facilitate the cross-shelf exchange of water masses and contribute to mixing, hence influencing the hydrographic properties of both the cold outflow and warm inflow.

*Acknowledgements.* For deployment and recovery of moorings, we would like to thank AWI and the crew and scientists on RV *Polarstern* cruises PS08 (recovery of moorings D1, D2, S2-1985 and S3), PS12 (deployment S2-1987), PS34 (deployment Fr1 and Fr2), PS53 (recovery F1–4) and PS82 (recovery SB, SC, SD and SE). Thanks to K. Brink for sharing the numerical code and I. Fer for helpful comments and suggestions. We would also like to thank two anonymous reviewers and L. Padman as well as the editor J. Huthnance for constructive comments which significantly improved the manuscript. The research was partially funded by the Centre for Climate Dynamics at the Bjerknes Centre.

## References


Årthun, M., Nicholls, K. W., Makinson, K., Fedak, M. A., and Boehme, L.: Seasonal inflow of warm water onto the southern Weddell Sea continental shelf, Antarctica, Geophysical Research Letters, 39, doi:10.1029/2012GL052856, http://doi.wiley.com/10.1029/2012GL052856, 2012.

Boehme, L., Lovell, P., Biuw, M., Roquet, F., Nicholson, J., Thorpe, S. E., Meredith, M. P., and Fedak, M.: Technical Note: Animal-borne CTD-Satellite Relay Data Loggers for real-time oceanographic data collection, Ocean Sci., 5, 685–695, doi:10.5194/os-5-685-2009, 2009.

Brink, K. H.: Coastal-trapped waves and wind-driven currents over the continental shelf, Annu. Rev. Fluid Mech., 23, 389–412, doi:10.1146/annurev.fl.23.010191.002133, 1991.

Brink, K. H.: Coastal-Trapped Waves with Finite Bottom Friction, Dyn. Atmos. Oceans, 41, 172–190, doi:10.1016/j.dynatmoce.2006.05.001, 2006.

British Antarctic Survey: UK Antarctic Surface Meteorology; 1947–2013, Database, Version 1.0, Polar Data Centre, British Antarctic Survey, http://dx.doi.org/10.5285/569d53fb-9b90-47a6-b3ca-26306e696706, 2013, updated 2014.

Cartwright, D. E.: Extraordinary Tidal Currents near St Kilda, Nature, 223, 928–932, doi:10.1038/223928a0, 1969.

Chapman, D. C.: Enhanced subinertial diurnal tides over isolated topographic features, Deep Sea Research Part A. Oceanographic Research Papers, 36, 815–824, doi:10.1016/0198-0149(89)90030-7, http://linkinghub.elsevier.com/retrieve/pii/0198014989900307, 1989.

Crawford, W. and Thomson, R.: Continental Shelf Waves of Diurnal Period Along Vancouver Island, Journal of Geophysical Research, 87, 9516–9522, http://onlinelibrary.wiley.com/doi/10.1029/JC087iC12p09516/full, 1982.

Darelius, E., Smedsrud, L. H., Østerhus, S., Foldvik, A., and Gammelsrød, T.: Structure and variability of the Filchner overflow plume, Tellus A, 61A, 446–464, doi:10.1111/j.1600-0870.2009.00391.x, http://tellusa.net/index.php/tellusa/article/view/15559http://onlinelibrary.wiley.com/doi/10.1111/j.1600-0870.2009.00391.x/full, 2009.

Darelius, E., Strand, K. O., Østerhus, S., Gammelsrød, T., Årthun, M., and Fer, I.: On the Seasonal Signal of the Filchner Overflow, Weddell Sea, Antarctica, Journal of Physical Oceanography, 44, 1230–1243, doi:10.1175/JPO-D-13-0180.1, http://journals.ametsoc.org/doi/abs/10.1175/JPO-D-13-0180.1, 2014.

Darelius, E., Fer, I., and Nicholls, K. W.: Observed vulnerability of Filchner-Ronne Ice Shelf to wind-driven inflow of warm deep water, Nature communications, 7, 2016.

Fahrbach, E., Rohardt, G., and Krause, G.: The Antarctic Coastal Current in the southeastern Weddell Sea, Polar Biology, 12, 171–182, doi:10.1007/BF00238257, http://link.springer.com/10.1007/BF00238257, 1992.

Fer, I., Müller, M., and Peterson, A. K.: Tidal forcing , energetics , and mixing near the Yermak Plateau, Ocean Science, 11, 287–304, doi:10.5194/os-11-287-2015, 2015.

Fer, I., Darelius, E., and Daae, K. B.: Observations of energetic turbulence on the Weddell Sea continental slope, Geophysical Research Letters, pp. 760–766, doi:10.1002/2015GL067349, http://dx.doi.org/10.1002/2015GL067349, 2015GL067349, 2016.

Foldvik, A. and Kvinge, T.: Bottom Currents in the Weddell Sea, Geophysical Institute Rep. No. 37, University of Bergen, 1974.

Foldvik, A., Gammelsrød, T., and Tørresen, T.: Circulation and water masses on the southern Weddell Sea shelf, Antarctic Research Series, 43, 5–20, doi:10.1029/AR043p0005, 1985a.

Foldvik, A., Kvinge, T., and Tørresen, T.: Bottom currents near the continental shelf break in the Weddell Sea, Oceanology of the Antarctic Continental Shelf, 43, doi:10.1029/AR043p0021, 1985b.

Foldvik, A., Middleton, J. H., and Foster, T. D.: The tides of the southern Weddell Sea, Deep Sea Research Part A. Oceanographic Research Papers, 37, 1345–1362, doi:10.1016/0198-0149(90)90047-Y, http://linkinghub.elsevier.com/retrieve/pii/019801490090047Y, 1990.

Foldvik, A., Gammelsrød, T., Østerhus, S., Fahrbach, E., Rohardt, G., Schröder, M., Nicholls, K. W., Padman, L., and Woodgate, R. A.: Ice shelf water overflow and bottom water formation in the southern Weddell Sea, Journal of Geophysical Research, 109, doi:10.1029/2003JC002008, http://doi.wiley.com/10.1029/2003JC002008http://onlinelibrary.wiley.com/doi/10.1029/2003JC002008/full, 2004.

Foreman, M.: Manual for Tidal Currents Analysis and Prediction, Pacific Marine Science Report 78-6, Institute of Ocean Sciences, Patricia Bay, Sidney, British Columbia, 1978.

Foster, T. D. and Carmack, E. C.: Frontal zone mixing and Antarctic Bottom Water formation in the southern Weddell Sea, Deep-Sea Research, 23, 301–317, 1976.

Gill, A. E.: Circulation and bottom water production in the Weddell Sea, Deep-Sea Research, 20, 111–140, doi:10.1016/0011-7471(73)90048-X, 1973.

Gordon, R. L. and Huthnance, J. M.: Storm-driven continental shelf waves over the Scottish continental shelf, Continental Shelf Research, 7, 1015–1048, doi:10.1016/0278-4343(87)90097-5, http://linkinghub.elsevier.com/retrieve/pii/0278434387900975, 1987.

Graham, J. A., Heywood, K. J., Chavanne, C. P., and Holland, P. R.: Seasonal variability of water masses and transport on the Antarctic continental shelf and slope in the southeastern Weddell Sea, Journal of Geophysical Research: Oceans, 118, 2201–2214, doi:10.1002/jgrc.20174, http://doi.wiley.com/10.1002/jgrc.20174, 2013.

Heath, R. A.: Tidal currents in the southwestern Pacific Basin and Campbell Plateau, southeast of New Zealand, Deep Sea Research Part A. Oceanographic Research Papers, 30, 393–409, doi:10.1016/0198-0149(83)90074-2, http://linkinghub.elsevier.com/retrieve/pii/0198014983900742, 1983.

Hellmer, H. H., Kauker, F., Timmermann, R., Determann, J., and Rae, J.: Twenty-first-century warming of a large Antarctic ice-shelf cavity by a redirected coastal current, Nature, 485, 225–228, doi:10.1038/nature11064, http://www.nature.com/nature/journal/v485/n7397/abs/nature11064.html, 2012.

Heywood, K. J., Locarnini, R. A., Frew, R. D., Dennis, P. F., and King, B. A.: Transport and water masses of the Antarctic Slope Front system in the eastern Weddell Sea, Ocean, ice, and atmosphere: Interactions at the Antarctic continental margin, Antarctic Research Series, 75, 203–214, http://onlinelibrary.wiley.com/doi/10.1029/AR075p0203/summary, 1998.

Hunkins, K.: Anomalous diurnal tidal currents on the Yermak Plateau, Journal of Marine Research, 44, 51–69, doi:10.1357/002224086788460139, http://openurl.ingenta.com/content/xref?genre=article&issn=0022-2402&volume=44&issue=1&spage=51, 1986.

Huthnance, J. M.: On the diurnal tidal currents over Rockall Bank, Deep Sea Research, 21, 23–35, doi:10.1016/0011-7471(74)90016-3, 1974.

Huthnance, J. M.: Circulation, exchange and water masses at the ocean margin: the role of physical processes at the shelf edge, Progress in Oceanography, 35, 353–431, doi:10.1016/0079-6611(95)80003-C, 1995.

Huthnance, J. M., Mysak, L. A., and Wang, D.-P.: Coastal trapped waves, in: Baroclinic Processes on Continental Shelves, edited by Mooers, C. N., vol. 3, American Geophysical Union, Washington, D. C., doi:10.1029/CO003p0001, 1986.

Jensen, M. F., Fer, I., and Darelius, E.: Low frequency variability on the continental slope of the southern Weddell Sea, Journal of Geophysical Research: Oceans, 118, 1–17, doi:10.1002/jgrc.20309, http://doi.wiley.com/10.1002/jgrc.20309, 2013.

Kida, S.: The Impact of Open Oceanic Processes on the Antarctic Bottom Water Outflows, Journal of Physical Oceanography, 41, 1941–1957, doi:10.1175/2011JPO4571.1, 2011.

Mack, S., Padman, L., and Klinck, J.: Extracting tidal variability of sea ice concentration from AMSR-E passive microwave single-swath data: a case study of the Ross Sea, Geophysical Research Letters, 40, 547–552, doi:10.1002/grl.50128, http://doi.wiley.com/10.1002/grl.50128, 2013.

Marques, G. M., Padman, L., Springer, S. R., Howard, S. L., and Özgökmen, T. M.: Topographic vorticity waves forced by Antarctic dense shelf water outflows, Geophysical Research Letters, 41, 1247–1254, doi:10.1002/2013GL059153, http://doi.wiley.com/10.1002/2013GL059153, 2014.

Meier, W., Fetterer, F., Savoie, M., Mallory, S., Duerr, R., and Stroeve, J.: NOAA/NSIDC Climate Data Record of Passive Microwave Sea Ice Concentration, Version 2, http://dx.doi.org/10.7265/N55M63M1, Boulder, Colorado USA. NSIDC: National Snow and Ice Data Center. Date accessed: 15/11/2016, 2013, updated 2015.

Middleton, J. H., Foster, T. D., and Foldvik, A.: Diurnal Shelf Waves in the Southern Weddell Sea, Journal of Physical Oceanography, 17, 784 – 791, http://dx.doi.org/10.1175/1520-0485(1987)017<0784:DSWITS>2.0.CO;2, 1987.

Mysak, L. A.: Recent Advances in Shelf Wave Dynamics, Reviews of Geophysics and Space Physics, 18, 211–241, doi:10.1029/RG018i001p00211, 1980.

Nakayama, Y., Ohshima, K. I., and Fukamachi, Y.: Enhancement of Sea Ice Drift due to the Dynamical Interaction between Sea Ice and a Coastal Ocean, Journal of Physical Oceanography, pp. 179–192, doi:10.1175/JPO-D-11-018.1, 2012.

Nicholls, K. W., Østerhus, S., Makinson, K., Gammelsrød, T., and Fahrbach, E.: Ice-ocean processes over the continental shelf of the southern Weddell Sea, Antarctica: a review, Reviews of Geophysics, 47, doi:10.1029/2007RG000250.1.INTRODUCTION, 2009.

Nøst, O. A., Biuw, M., Tverberg, V., Lydersen, C., Hattermann, T., Zhou, Q., Smedsrud, L. H., and Kovacs, K. M.: Eddy overturning of the Antarctic Slope Front controls glacial melting in the Eastern Weddell Sea, Journal of Geophysical Research, 116, doi:10.1029/2011JC006965, http://doi.wiley.com/10.1029/2011JC006965, 2011.

Núñez-Riboni, I. and Fahrbach, E.: Seasonal variability of the Antarctic Coastal Current and its driving mechanisms in the Weddell Sea, Deep Sea Research Part I: Oceanographic Research Papers, 56, 1927–1941, doi:10.1016/j.dsr.2009.06.005, http://linkinghub.elsevier.com/retrieve/pii/S0967063709001344, 2009.

Ono, J., Ohshima, K. I., Mizuta, G., Fukamachi, Y., and Wakatsuchi, M.: Diurnal coastal-trapped waves on the eastern shelf of Sakhalin in the Sea of Okhotsk and their modification by sea ice, 28, 697–709, doi:10.1016/j.csr.2007.11.008, 2008.

Orsi, A. H., Johnson, G. C., and Bullister, J. L.: Circulation, mixing, and production of Antarctic Bottom Water, Progress in Oceanography, 43, 55–109, doi:10.1016/S0079-6611(99)00004-X, 1999.

Padman, L. and Kottmeier, C.: High-frequency ice motion and divergence in the Weddell Sea, Journal of Geophysical Research, 105, 3379–3400, doi:10.1029/1999JC900267, 2000.

Padman, L., Plueddemann, A. J., Muench, R. D., and Pinkel, R.: Diurnal tides near the Yermak Plateau, Journal of Geophysical Research, 97, 12 639–12 652, doi:10.1029/92JC01097, 1992.

Padman, L., Fricker, H. A., Coleman, R., Howard, S., and Erofeeva, L.: A new tide model for the Antarctic ice shelves and seas, Annals of Glaciology, 34, 247–254, doi:10.3189/172756402781817752, 2002.

Pawlowicz, R., Beardsley, B., and Lentz, S.: Classical tidal harmonic analysis including error estimates in MATLAB using T_TIDE, Computers & Geosciences, 28, 929–937, doi:10.1016/S0098-3004(02)00013-4, http://linkinghub.elsevier.com/retrieve/pii/S0098300402000134, 2002.

Pereira, A. F., Beckmann, A., and Hellmer, H. H.: Tidal Mixing in the Southern Weddell Sea: Results from a Three-Dimensional Model, Journal of Physical Oceanography, 32, 2151–2170, http://dx.doi.org/10.1175/1520-0485(2002)032<2151:TMITSW>2.0.CO;2, 2002.

Saint-Guily, B.: Sur la propagation des ondes de seconde classe le long d'un talus continental, C. R. Acad. Sci. Paris, 282, 1976.

Skarðhamar, J., Skagseth, Ø., and Albretsen, J.: Diurnal tides on the Barents Sea continental slope, Deep Sea Research I, 97, 40–51, doi:10.1016/j.dsr.2014.11.008, http://linkinghub.elsevier.com/retrieve/pii/S096706371400212X, 2015.

St-Laurent, P., Klinck, J. M., and Dinnimann, M. S.: On the Role of Coastal Troughs in the Circulation of Warm Circumpolar Deep Water on Antarctic Shelves, Journal of Physical Oceanography, 43, 51–64, doi:10.1175/JPO-D-11-0237.1, 2013.

Stull, R. B.: An introduction to boundary layer meteorology, vol. 13, Springer Science & Business Media, doi:10.1007/978-94-009-3027-8, 2012.

Sverdrup, H. U.: The currents off the coast of Queen Maud Land, Særtrykk av Norsk Geografisk Tidsskrift, 14, 239–249, doi:10.1080/00291955308551737, 1953.

Thomson, R. E. and Crawford, W. R.: The Generation of Diurnal Period Shelf Waves by Tidal Currents, Journal of Physical Oceanography, 12, 635–643, http://dx.doi.org/10.1175/1520-0485(1982)012<0635:TGODPS>2.0.CO;2, 1982.

Wang, D.-P. and Mooers, C. N.: Coastal-Trapped Waves in a Continuously Stratified Ocean, Journal of Physical Oceanography, 6, 853 – 863, http://dx.doi.org/10.1175/1520-0485(1976)006<0853:CTWIAC>2.0.CO;2, 1976.

Wang, Q., Danilov, S., Fahrbach, E., Schröter, J., and Jung, T.: On the impact of wind forcing on the seasonal variability of Weddell Sea Bottom Water transport, Geophysical Research Letters, 39, doi:10.1029/2012GL051198, 2012.

Welch, P. D.: The use of fast Fourier transform for the estimation of power spectra: a method based on time averaging over short, modified periodograms, IEEE Transactions on Audio and Electroacoustics, 2, 70–73, 1976.

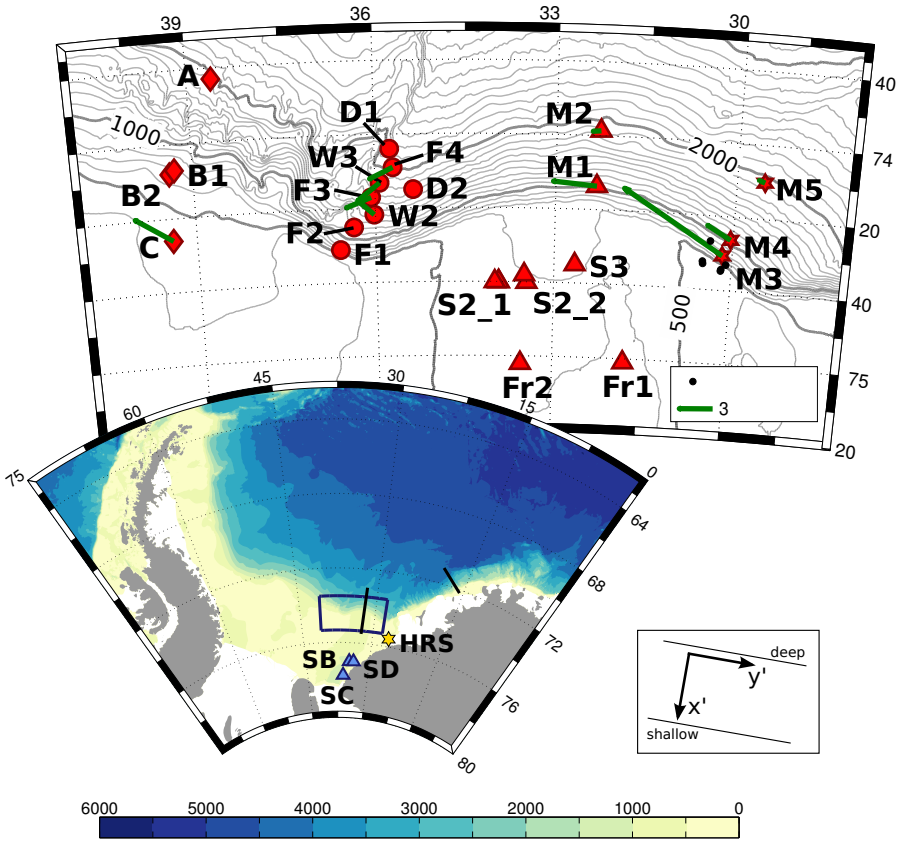


**Figure 1.** Map of the Weddell Sea (bathymetry from The GEBCO_2014 Grid, version 20150318, http://www.gebco.net) and locations of moorings in the study area (shapes according to their location west, along the ridge, at and in the Filchner Depression, or east on the continental slope). S2_1 and S2_2 show the location of mooring S2 prior to and after 2000. Annual mean currents (see Sect. 2) are indicated by green arrows. The study area is also the area the sea ice concentration has been averaged over. The yellow star marks Halley Research Station (HRS), while the two black lines indicate cross-slope sections used for the bathymetry test in the numerical code and to derive diurnal tidal KE from the tidal model CATS. The inset in the lower right corner illustrates the rotation of the coordinate system.

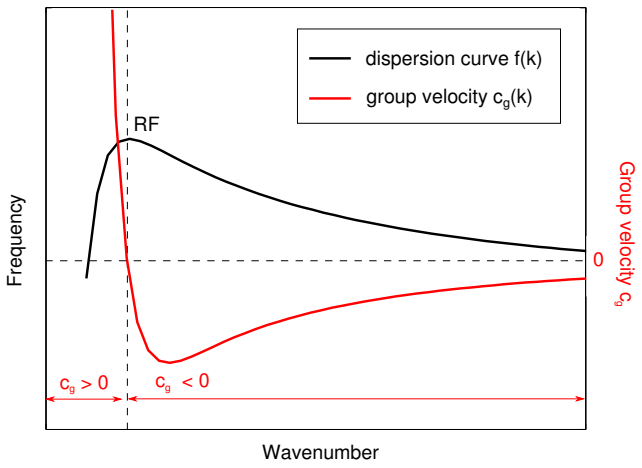


**Figure 2.** Illustration of a typical mode 1 CTW dispersion curve (black line) with the corresponding group velocity (red line). For small wavenumbers, the group velocity is positive, while it becomes negative for larger wavenumbers, i.e. indicating a change of direction of energy propagation. At the maximum of the dispersion curve (the resonant frequency, or "RF"), the group velocity vanishes and energy is trapped.

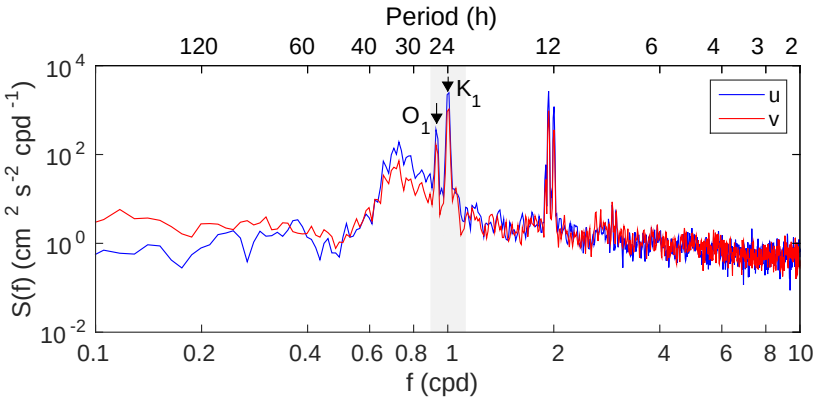


**Figure 3.** Power spectral density of depth-averaged, rotated $u$- and $v$-velocity components at mooring M3. The diurnal tidal frequency band around one cycle per day (cpd) is marked in grey; black arrows indicate frequencies of the $K_1$ and $O_1$ tidal constituents.

**Table 1.** Name, recording year, location in degrees and minutes, bottom depth, number of recording days, depths of current meters or ADCPs (in format "first level:depth increment:last level") in metres above bottom (m.a.b.) and angle $\beta$ for the clockwise rotation of the coordinate system for all moorings used in this study. For some moorings located on the flat shelf or close to varying bathymetry (i.e. at the ridge), the rotation angles have increased uncertainty (marked with an asterisk). More details on the moorings can be found in Foldvik et al. (2004) and references therein, as well as in Jensen et al. (2013) and Darelius et al. (2016).

| Mooring | Year | Latitude | Longitude | Depth (m) | Recording days | Instrument depth (m.a.b.) | $\beta$ |
|---|---|---|---|---|---|---|---|
| B1 | 1968 | -74 07 | -39 18 | 657 | 265 | 23 | 122 |
| B2 | 1968 | -74 08 | -39 23 | 663 | 460 | 23 | 122 |
| S2-1977 | 1977 | -74 40 | -33 56 | 558 | 411, 257 | 25, 100 | -10* |
| C | 1977 | -74 26 | -39 24 | 475 | 630, 631 | 25, 125 | 127 |
| A | 1978 | -73 43 | -38 36 | 1939 | 65, 440 | 25, 125 | 123 |
| S2-1985 | 1985 | -74 40 | -33 56 | 545 | 371, 283, 258 | 25, 100, 190 | -10* |
| D1 | 1985 | -74 04 | -35 45 | 2100 | 352 | 25, 100 | 13* |
| D2 | 1985 | -74 15 | -35 22 | 1800 | 281, 52 | 25, 100 | 70* |
| S2-1987 | 1987 | -74 40 | -34 00 | 558 | 352, 407 | 25, 100 | -10* |
| S3 | 1992 | -74 35 | -32 39 | 659 | 165, 356 | 70, 170 | -10* |
| Fr1 | 1995 | -75 01 | -31 46 | 610 | 691, 837, 828, 828 | 20, 126, 232, 353 | 50* |
| Fr2 | 1995 | -75 02 | -33 33 | 574 | 683, 837, 829, 829 | 20, 126, 232, 383 | 25 |
| F1 | 1998 | -74 31 | -36 36 | 647 | 327, 277, 393 | 10, 56, 207 | 124 |
| F2 | 1998 | -74 25 | -36 22 | 1180 | 309, 390, 326, 348 | 10, 56, 202, 433 | 106 |
| F3 | 1998 | -74 17 | -36 04 | 1637 | 395 | 56, 413 | 94 |
| F4 | 1998 | -74 09 | -35 42 | 1984 | 376, 390, 332 | 10, 56, 207 | 90 |
| S2-2003 | 2003 | -74 40 | -33 28 | 596 | 421 | 25, 100 | -10* |
| M1 | 2009 | -74 13 | -32 19 | 967 | 365 | 25, 46 | 110 |
| M2 | 2009 | -73 58 | -32 16 | 1898 | 364 | 19, 78:4:150 | 110 |
| M3 | 2009 | -74 30 | -30 09 | 725 | 361 | 25, 123:4:1993, 10:5:505 | 110 |
| M4 | 2009 | -74 26 | -30 02 | 1051 | 361 | 25, 442:16:986 | 110 |
| M5 | 2009 | -74 10 | -29 32 | 1917 | 361, 336 | 26, 55:16:391 | 110 |
| S2-2010 | 2010 | -74 38 | -33 30 | 612 | 363 | 25, 104, 176 | -10* |
| W2 | 2010 | -74 23 | -36 01 | 1411 | 361, 344, 302, 318 | 25, 84, 194:4:234, 289:4:389 | 94 |
| W3 | 2010 | -74 13 | -35 55 | 1488 | 363, 363, 91, 304 | 25, 93, 163:2:209, 216:4:272 | 97 |
| SB | 2013 | -77 00 | -34 28 | 705 | 371 | 51:8:395 | 37 |
| SC | 2013 | -77 45 | -36 09 | 700 | 376 | 26:4:214 | 28 |
| SD | 2013 | -77 00 | -34 03 | 505 | 371 | 19:4:119 | 37 |
| SE | 2013 | -77 01 | -34 14 | 590 | 196 | 175 | 37 |

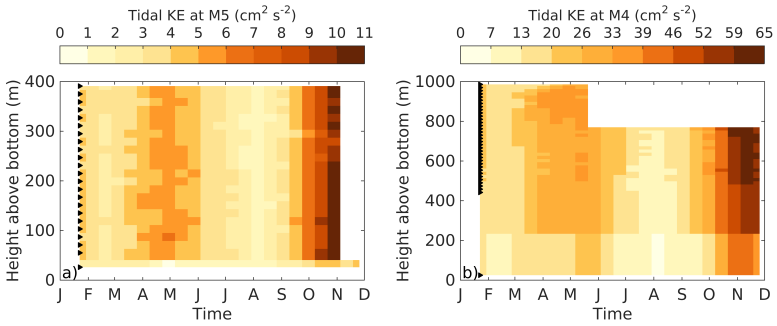


**Figure 4.** Diurnal tidal KE over time and depth at a) mooring M5 and b) mooring M4 on the continental slope, located above the 1900 m and 1050 m isobath, respectively. Black triangles mark the depths of individual measurements. Note the different scale for diurnal tidal KE and vertical axis in a) and b).

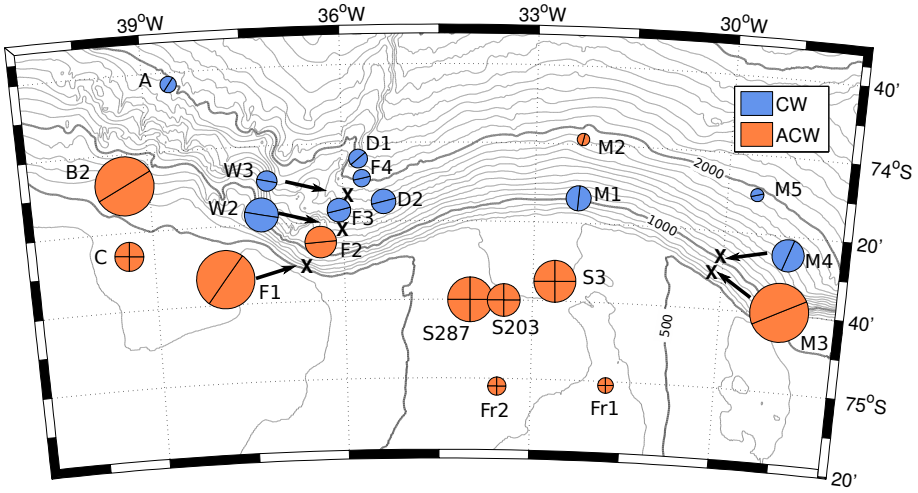


**Figure 5.** Map showing the maximum depth-averaged, diurnal tidal KE reached in austral summer. The area of the circles is proportional to the square root of the KE. Blue circles indicate a clockwise (CW) rotation of tidal currents at the $K_1$ frequency, red circles an anticlockwise (ACW) rotation. The line through the circles indicates the orientation of the major axis (i.e. strongest tidal current). Tidal current ellipses with an aspect ratio (semi-minor/semi-major axis) of more than 0.8, i.e. close to circular, are marked with two crossing lines instead of a single line. At the location of mooring S2 with five years of measurements, the data for the deployment years 1987 (S287) and 2003 (S203) are presented. Some circles are displaced from their actual mooring locations (marked with "X") for legibility.

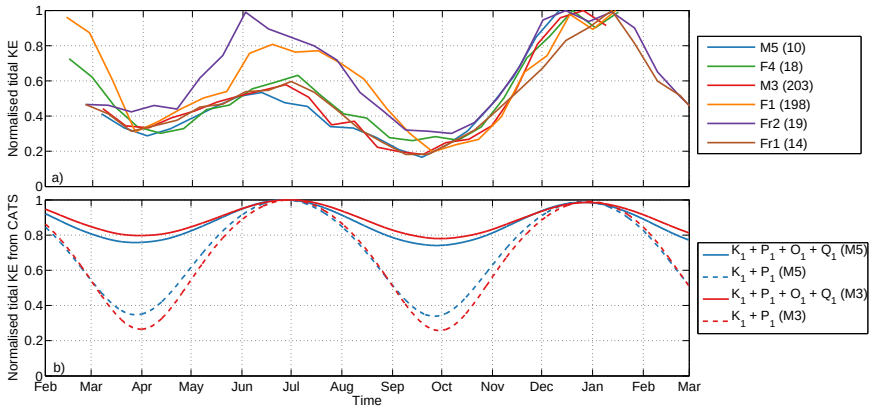


**Figure 6.** a) Time series of normalised diurnal tidal KE at moorings M5 and F4 (deeper continental slope), M3 and F1 (shelf break) and the first year of record at Fr2 and Fr1 (shelf). At M5, KE is only calculated until the ADCP stops measuring (see Table 1). The maximum diurnal tidal KE values in $cm^2\,s^{-2}$ are given in parentheses in the legend. b) Time series of normalised tidal KE at the $K_1$+$P_1$ and $K_1$+$P_1$+$O_1$+$Q_1$ tidal frequencies as predicted by the CATS tidal model at the locations and deployment times of moorings M3 and M5.

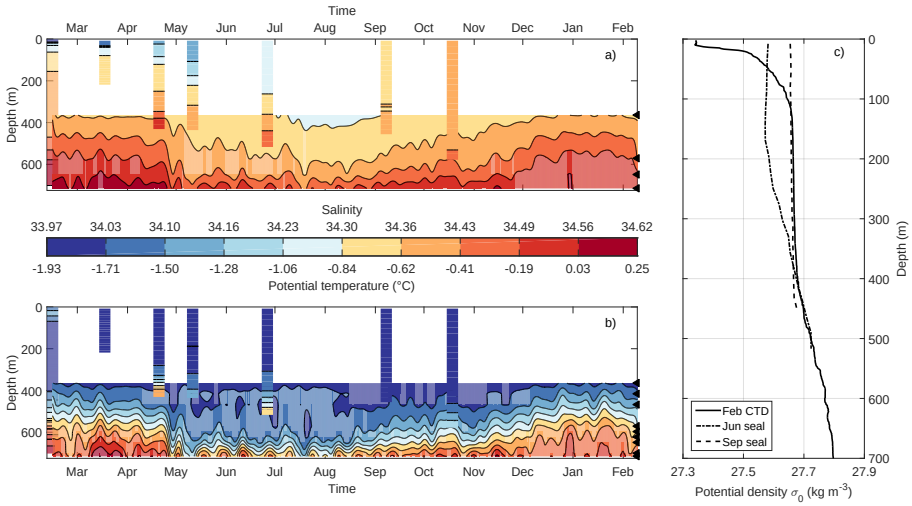


**Figure 7.** Hovmöller diagrams for a) salinity and b) temperature. The continuous records below approximately 350 m depth are the hydrographic time series of moored instruments at M3, acquired in 2009 (see Table 1). The mooring data have been low-pass filtered by applying a fourth order Butterworth filter removing variability at shorter periods than the cut-off period of 168 h (one week). Black triangles mark the depths of individual measurements. CTD profiles from ship (from the deployment cruise of mooring M3 in 2009, first profile) and seals (obtained in 2011 from within approximately 10 km distance to mooring M3, see Fig. 1) complement the mooring records. The width of the profiles is arbitrarily set to one week for clarity. Panel c) shows the seasonal development of potential density based on three of the temperature and salinity profiles near mooring M3.

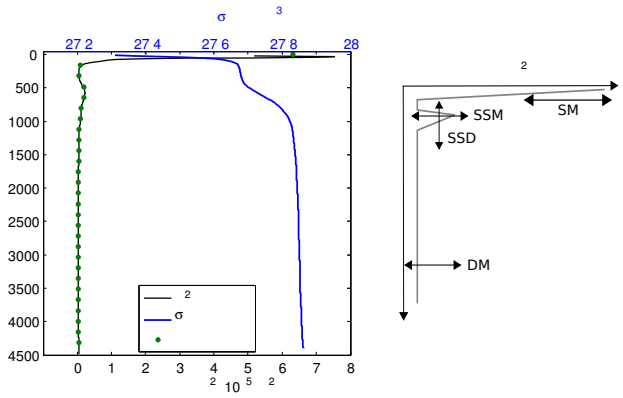


**Figure 8.** a) Profiles of potential density (blue line) and resulting stratification ("reference stratification", black line) from historic CTD data obtained in January and February in the area of moorings M1 to M5, merged with profiles from the deeper Weddell Sea at depth. Green markers indicate the vertical levels of the numerical code. b) Sketch showing the parameters changed in the stratification sensitivity tests. Arrows indicate direction (but not magnitude) of changes. SM: surface magnitude, SSM: subsurface magnitude, SSD: subsurface depth, DM: deep magnitude.

**Table 2.** Parameters of the reference stratification profile and corresponding ranges of change in the sensitivity test (SM: surface magnitude, SSM: subsurface magnitude, SSD: subsurface depth, DM: deep magnitude). For case DM, the average (av.) is given in addition to the range of values in the profile section.

| | SM, $10^{-5}\,s^{-2}$ | SSM, $10^{-5}\,s^{-2}$ | SSD, m; model level | DM, $10^{-7}\,s^{-2}$ |
|---|---|---|---|---|
| reference stratification | 3.20 | 0.17 | 640; 5 | 1.99–4.42; av.: 2.92 |
| sensitivity test | 0.07–4.05 | 0.04–2.78 | 320–960; 3–7 | 1–30 |

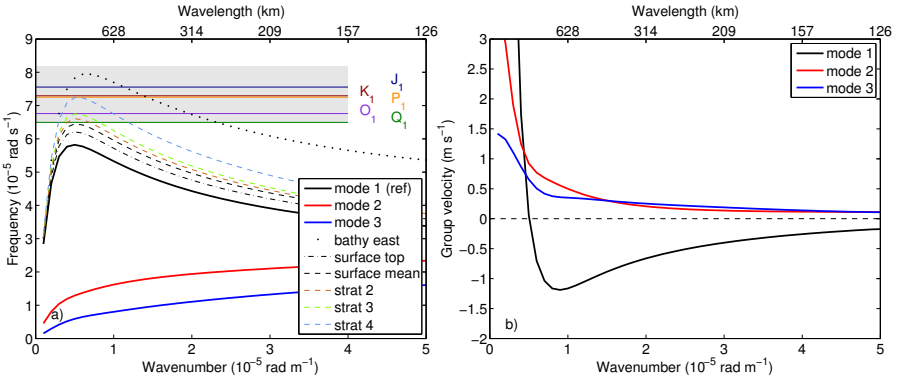


**Figure 9.** a) Dispersion curves for CTWs of modes 1–3 using the reference stratification (thick lines). In addition, the dispersion curves for mode 1 CTWs for the bathymetry east of the study area ("bathy east"), differently inferred surface $N^2$ values for the reference stratification ("surface top", using the uppermost value of the observational stratification profile, and "surface mean", using the average of the upper 80 m of the observed stratification profile) and three other stratification profiles are shown. Stratification profiles 2–4 are representative for regions in the study area with increasing distance west of the reference stratification and inferred similarly. The diurnal tidal band is shaded in light grey with the most important diurnal frequencies marked by coloured lines. b) Group velocities for CTWs of modes 1–3 using the reference stratification. Zero group velocity is indicated by a dashed line.

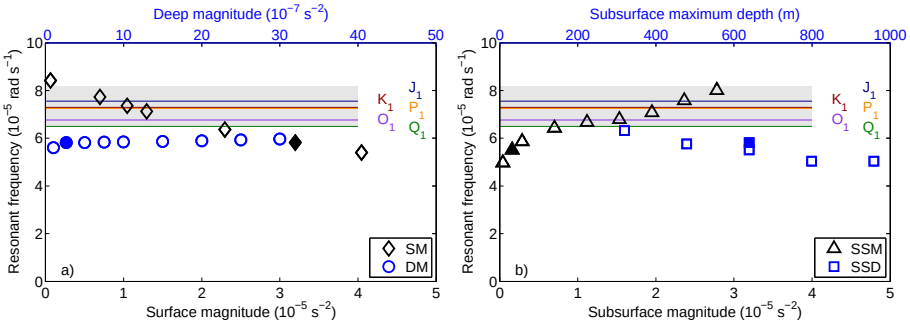


**Figure 10.** Sensitivity test for changing stratification. a) The surface magnitude (SM) and deep magnitude (DM) are varied. b) The subsurface magnitude (SSM) and its depth (SSD) are varied. Results from the reference stratification profile are indicated by filled markers. For case SSD, the shape of SSM in the profile is simplified (open marker below filled marker) and then varied in depth. The diurnal tidal band is shaded in light grey with the most important diurnal frequencies marked by coloured lines.

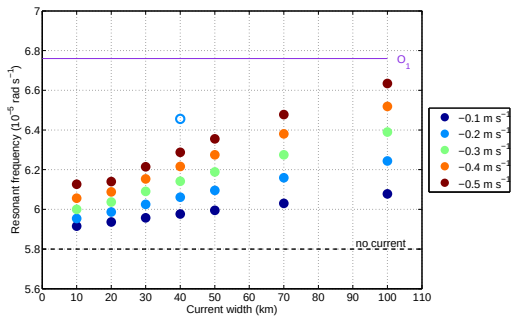


**Figure 11.** Sensitivity test for changing the width and strength of the slope current. Additionally, an example for the RF of a less barotropic (i.e. surface-enhanced) current is shown by the open blue marker. The RF for the reference stratification without added current (see Fig. 9) is indicated by a broken black line, and the tidal frequency $O_1$ is marked by a solid purple line.

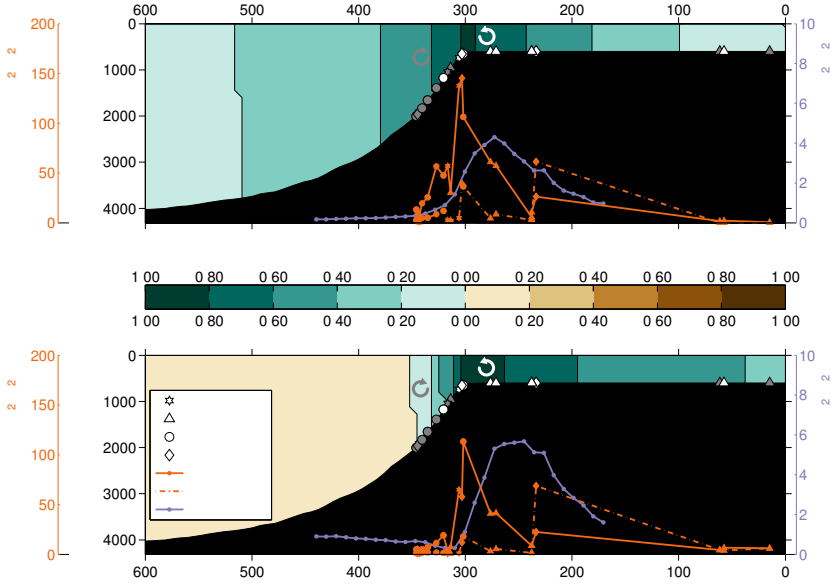

**Figure 12.** Normalised along-slope modal structure from the numerical code (background colours) at the wave number of the RF for reference stratification. Moorings within the modelled domain are indicated by markers whose shapes correspond to the geographic locations (west, ridge, Filchner Depression, east) as in Fig. 1. Markers filled in grey (white) indicate a clockwise (anticlockwise) rotational sense of the diurnal tidal currents. For each mooring location, diurnal tidal KE for austral summer is shown, both from observations (solid orange line) and derived from CATS (broken orange line). Diurnal tidal KE predicted from the CATS run along the cross-shelf section through the locations of moorings M1 and M2 (see Fig. 1 for location) is shown as purple line with markers indicating locations of predicted currents. Panel a) shows modal structure for $u$, b) modal structure for $v$; the legend is shared.

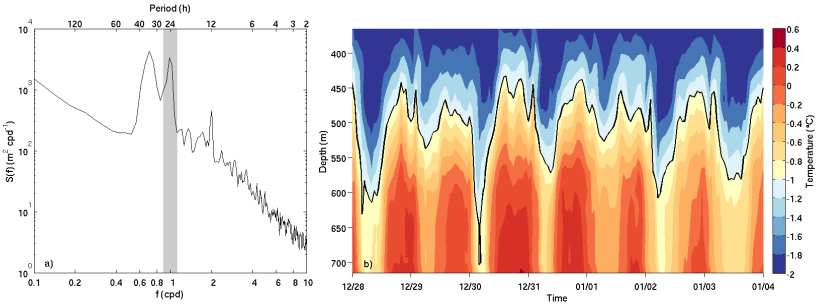


**Figure 13.** a) Power spectral density of the height above the bottom of the -1° C isotherm indicating the transition between WW and WDW at M3. The diurnal tidal frequency band is marked in grey. b) Hovmöller diagram of low-passed filtered temperature at mooring M3 from 28 December to 4 January. The -1° C isotherm is shown by a black line.

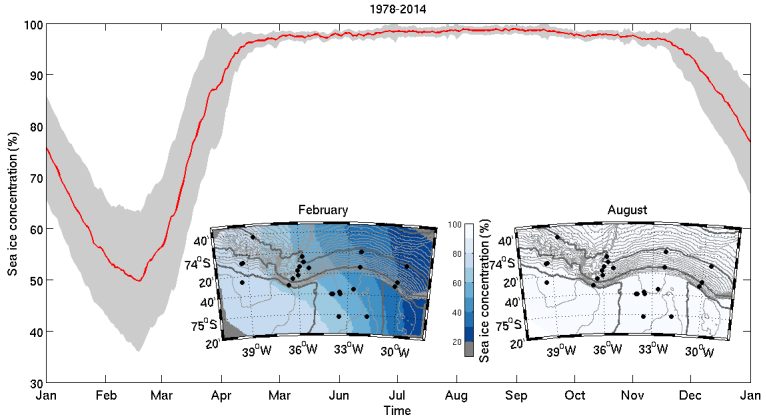


**Figure 14.** Sea ice concentration averaged over the study area and the period 1978-2014 (red line) with standard deviation (grey). Insets show maps of mean sea ice concentrations in February and August; isobaths and mooring locations (black dots) are as in Figure 1.